Master's Thesis 2013

Candidate: Nataliia Peresunko

Title: CO_2 capture solvent performance characterization

Telemark University College
Faculty of Technology
M.Sc. Programme

MASTER'S THESIS, COURSE CODE FMH606

Student: **Nataliia Peresunko**

Thesis title: CO_2 capture solvent performance characterization

Signature: ……

Number of pages: <76>

Keywords: CO_2, MEA, MPA,4-amino-1-butanol, 5-amino-1 pentanol, equilibrium cell, gas chromatograph, $BaCl_2$ titration,CO_2 loading, uncertainty.

Supervisor: Klaus-J.Jens sign.: .....

2nd Supervisor: Zulkifli Bin Idris sign.: ……...

Censor: <name> sign.: ……...

External partner: <Dag Eimer, Tel-Tek> sign.: ……...

Availability: <Open/Secret>

Archive approval (supervisor signature)**:** sign.: …… **Date :**……

Abstract:

The aim of this work is to determine partial pressures and CO_2 loadings of primary amine aqueous solutions such as monoethanolamine, 3-amino-1-propanol, 4-amino-1-butanol and 5-amino-1-pentanol at the equal vapor liquid equilibrium conditions. Concentrations of all investigated aqueous amine solutions were kept at 30(wt)%. The temperature during the experiments was maintained 40^0C at close to atmospheric pressure, and CO_2 loadings in the range 0.2-0.5mole CO_2/mole amine.

The literature review of previous works in regard to VLE in CO_2-water-amine systems specifically for monoethanolamine, 3-amino-1-propanol, 4-amino-1-butanol and 5-amino-1-pentanol was carried out. The issue of the influence of structural change of amines on their capture capacities was studied in the work likewise. Literature review revealed the dependence of amine structures on CO_2 loading in absorption and desorption processes.

The experiments were run using an equilibrium cell connected to the gas chromatograph. Gas chromatograph was calibrated with CO_2 gases correspondently to CO_2 loading. The time 1 hour was permitted for CO_2 absorption to ensure vapor liquid equilibrium conditions in CO_2-water-amine system. Partial pressure of amines was analyzed after the extraction of the samples from equilibrium cell closed loop to gas chromatograph.

CO_2 loadings were analyzed with $BaCl_2$ titration method. From two to three parallels of each sample were used to carry out the analysis.

Uncertainty analysis of CO_2 partial pressures and CO_2 loadings was performed for all amines.

Estimated vapor-liquid equilibrium curves of all amines were compared with each other. It was concluded that the cyclic capacities of investigated amines have reverse relationship to the increase of amine carbon chain length, in spite of the fact that absolute loading capacity increases with the increase of the number of carbons in carbon chain.

Table of contents

PREFACE **5**

NOMENCLATURE **6**

OVERVIEW OF TABLES AND FIGURES **7**

1 INTRODUCTION **9**

1.1 GLOBAL PROBLEM OF CO_2 EMISSIONS 9
1.2 CO_2 CAPTURE TECHNOLOGIES OVERVIEW 10
1.3 ABSORBENTS OVERVIEW 12
1.3.1 Alkanolamine family *12*
1.3.2 Monoethanolamine *14*
1.3.3 Relationship between structure of amines and CO_2 absorption capacity *14*
1.4 OUTLINE OF THE THESIS 15

2 LITERATURE RESEARCH **17**

2.1 PREVIOUS VAPOR-LIQUID- EQUILIBRIUM STUDIES OF AMINE-WATER- CO_2 SYSTEMS 17
2.1.1 Monoethanolamine *17*
2.1.2 5-amino-1-pentanol, 4-amino-1-butanol and 3-amino -1-pentanol *17*
2.2 INFLUENCE OF STRUCTURAL CHANGE OF AMINES ON THEIR CO_2 CAPTURE ACTIVITIES . 20

3 SOLUBILITY OF CO_2 IN ALKANOLAMINES **23**

3.1 INTRODUCTION 23
3.1.1 Gas chromatography *23*
3.1.2 Titration *24*
3.2 MATERIALS 25
3.3 EQUILIBRIUM CELL APPARATUS DESIGN 25
3.4 MEASUREMENT OF CO_2 PARTIAL PRESSURE IN THE GAS PHASE 30
3.5 MEASUREMENT OF CO_2 LOADING AND AMINE CONCENTRATION IN THE LIQUID PHASE . 32
3.5.1 CO_2 loading measurement *33*
3.5.2 CO_2 concentration measurement *34*
3.5.3 CO_2 loading and amine concentration calculation *35*

4 UNCERTAINTY ANALYSIS **37**

4.1 INTRODUCTION 37
4.2 UNCERTAINTY ANALYSIS FOR MEASURED VALUES OF CO_2 PARTIAL PRESSURE IN GAS SAMPLES 38
4.3 UNCERTAINTY ANALYSIS FOR VALUES OF CO_2 LOADINGS IN LIQUID SAMPLES OBTAINED WITH $BaCl_2$ TITRATION METHOD 40

4.3.1 Uncertainty of amine concentration *40*
4.3.2 Uncertainty of the loading analysis *44*

5 RESULTS AND DISCUSSION **48**

6 CONCLUSION **57**

7 SUGGESTION FOR FURTHER WORK **58**

REFERENCES **59**

APPENDICES **62**

Preface

I would like to thank my supervisor, Klaus Joachim Jens for his guidance and invaluable support during this course.

I will also like to extend my gratitude to my co-supervisor Zulkifli Bin Idris for his unlimited support and guidance in laboratoty experiments.

My deep gratitude to Dag Eimer from Tel-Tek for his guidance in answering many theotretical questions.

My special thanks to Chameera Jayarathna from Tel-Tek and Henrik Jilvero from Chalmers University of Technology, for their great favors in experimental work.

My sincere gratitude also goes to Anita Elverhøy, Tel-Tek, whose experimental and uncertainty analysis methodology was adopted in this Master thesis.

Porsgrunn, 03th July 2013

Peresunko Nataliia

Nomenclature

AMP	2-amino-2-methyl-1-propanol;
4A1B	4-amino-1-butanol;
5A1P	5-amino-1-pentanol;
$BaCl_2$	barium chloride;
CCS	carbon capture and storage;
CO_2	carbon dioxide;
COS	carbonile sulfide;
DEA	diethanolamine;
DGA	diglycolamine;
DIPA	diisoprapanolamine;
GC	gas chromotograph;
HCl	hydrochloric acid;
MEA	monoethanolamine;
MDEA	methyldiethanolamine;
MPA	3-amino-1-propanol;
NO_2	nitrogen dioxide;
NaOH	sodium hydroxide
PE	2-piperidineethanol;
TEA	triethanolamine;
VLE	vapor-liquid equilibrium;
P_{CO2}	partial pressure of CO_2, kPa;
Rel. Std. Dev	related standard deviation,%;
$\frac{Uc(Y)}{Y}$	standard uncertainty;
Y	analytical result;
Uc	combined uncertainty;
U	expanded uncertainty;
C	concentration, mol/l;
V	volume,ml;
M	molar mass, g/mol;
n	number of mols, mol;
m	mass;
α	loading, mol CO_2/mol amine.

Overview of tables and figures

List of tables

Table 1-1: Alkanolamine-based absorbents investigated in this work. 15

Table 2-1: Literature review of 30 (wt) % MEA. 17

Table 2-2: Solubility of CO_2 in 2 mol·dm-3 MPA aqueous solutions at 40 °C temperature [34]. 19

Table 2-3: Solubility of CO_2 in 4 mol·dm-3 MPA aqueous solutions at 40 °C temperature [34]. 20

Table 3-1: Elements of the equilibrium cell. 28

Table 3-2: Valves used in the equilibrium cell system. 30

Table 5-1: Vapor liquid equilibrium data from this work for 30 % (wt) aqueous MEA at 40°C. 48

Table 5-2: Vapor liquid equilibrium data from this work for 30 % (wt) aqueous MPA at 40°C. 48

Table 5-3: Vapor liquid equilibrium data from this work for 30 % (wt) aqueous 4A1B at 40°C. 49

Table 5-4: Vapor liquid equilibrium data from this work for 30 % (wt) aqueous 5A1P at 40°C. 49

Table 5-5: Vapor liquid equilibrium data from Jayarathna et al. work for 30 % (wt) aqueous MEA at 40^0C. 49

List of figures

Figure 1-1: Global CO_2 emissions per region from fossil fuel and cement production [1]. 9

Figure 1-2:CO_2 emissions from energy and industry as defined in ETP 2012 [3]. 10

Figure 1-3: Post combustion CO_2 capture [6]. 11

Figure 1-4: Technology options for CO_2 separation and capture [7]. 12

Figure 2-1: Effect of chain length in alkanolamine-based solvents for 2.5 mole/L concentration [19]. 22

Figure 3-1: Schematic of a gas chromatograph [37]. 24

Figure 3-2: Strong acid titration curve [38]. 25

Figure 3-3: Schematic diagram of Equilibrium cell set-up. 26

Figure 3-4: Equilibrium cell apparatus. 27

Figure 3-5: Elements of equilibrium cell apparatus. 28
Figure 3-6: Laboratory equipment. 30
Figure 3-7: Gas chromatograph..... 32
Figure 3-8: Titrator Mettler Toledo T50. 33
Figure 3-9: Titration with 0.1M NaOH. 34
Figure 3-10: Titration with 1M HCl..... 34
Figure 5-1: CO_2 partial pressures of 30% (wt) aqueous MEA at 40°C for the CO_2 loadings range 0.2-0.6 mole CO_2/mole MEA. 50
Figure 5-2: CO_2 partial pressures of 30% (wt) aqueous MEA at 40°C for the CO_2 loadings range 0.3-0.6 mole CO_2 /mole MEA. 50
Figure 5-3: CO_2 partial pressures of 30% (wt) aqueous MEA at 40°C for the CO_2 loadings range 0.15-12 mole CO_2 /mole MEA. 51
Figure 5-4: CO_2 partial pressures of 30% (wt) aqueous MEA at 40°C for the CO_2 loadings range 0.3-0.65 mole CO_2 /mole MEA. 51
Figure 5-5: Equilibrium solubility, 30% (wt) aqueous MPA at 40°C..... 53
Figure 5-6: Equilibrium solubility, 30% (wt) aqueous MPA at 40°C..... 53
Figure 5-7: Equilibrium solubility, 30%(wt) aqueous MEA, MPA, 4A1B and 5A1P at 40^{0}C..... 54
Figure 5-8: Equilibrium solubility, 30%(wt) aqueous MEA, MPA, 4A1B and 5A1P at 40^{0}C at CO_2 partial pressure range 0-3.5 kPa. 55
Figure 5-9: Equilibrium solubility, 30%(wt) aqueous MEA, MPA, 4A1B and 5A1P at 40^{0}C at CO_2 partial pressure range 0-0.12 kPa. 56

1 Introduction

1.1 Global problem of CO_2 emissions

The trend of CO_2 emissions is increasing continuously. As can be seen from the Figure 1- 1, after the 1 % decrease in 2009, the level of emissions increased on 5% in 2010 [1]. Such situation is related to financial crisis and weak economic conditions of many countries [2].

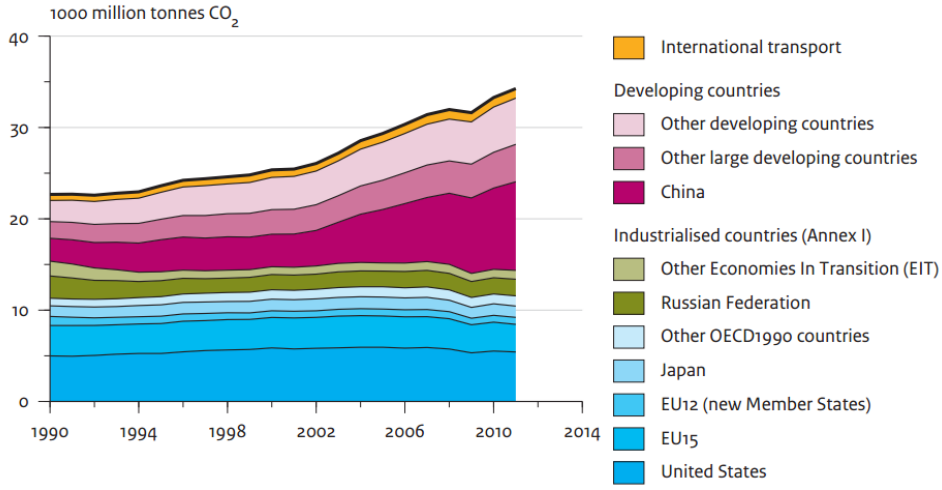

Figure 1-1: Global CO_2 emissions per region from fossil fuel and cement production [1].

The global warming has gained a lot of attention in recent years and, is directly associated with the problem of CO_2 emissions. According to the International Environmental Agency [3], countries can follow three effect scenarios for global CO_2 emissions, represented in a Figure 1-2. Complete neglect of the problem is predicted in 6D scenario, leads to double increase in CO_2 emissions and average temperature increase of 6 ^{o}C in the World by 2050 compared to 2010. However, following a 2D scenario, intensive actions at both governmental and industrial levels, will contribute to two times decrease in global CO_2 emissions with average temperature increase of 2 ^{o}C. Average temperature increase on 4 ^{o}C is expected if countries follow 4D scenario.

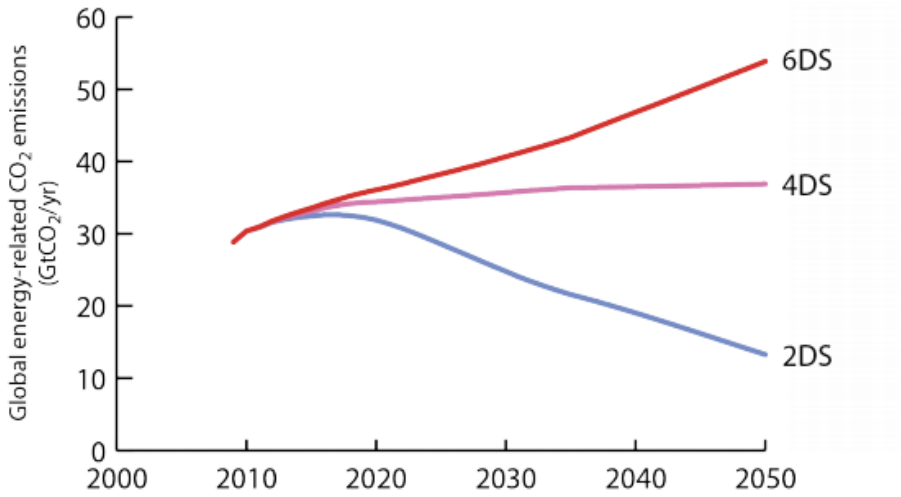

Figure 1-2:CO_2 emissions from energy and industry as defined in ETP 2012 [3].

Continuous research and development for the reduction of CO_2 emissions are being carried out by industries to meet the governmental requirements for the reduction of CO_2 emissions. Carbon capture and storage technologies (CCS) are currently dominant option to achieve significant results in solving the problem of CO_2 emissions [4]. CCS includes pre-combustion, oxy-fuel combustion and post-combustion technologies.

1.2 CO_2 capture technologies overview

The idea of pre-combustion technology is to separate CO_2 from the fuel before the combustion process. Fossil fuel and steam are converted in to CO_2 and H_2 in the reforming unit and then separated with scrubber column. Rich with H_2 gas can be further used as a fuel in power plant, thus CO_2 will not form in combustion process. Although pre-combustion CO_2 capture can clear up to 90% of CO_2 from the industry, the process has to be integrated into the combustion process and is expensive for the existing power plants. Thus pre-combustion technology is more convenient for new facilities. Furthermore the technology still requires considerable research and development.

Oxy-fuel combustion is a process where oxygen is used instead of air as oxidizer in combustion process. Oxygen is separated from air with air-separation unit prior to combustion. CO_2 and water vapor are products of combustion and can be easily separated by condensation process, which is the main advantage of the process. It is possible to achieve 100 % of CO_2 removal. However the air separation is an expensive process and is an obstacle for implementation of the oxy-fuel combustion. Oxy-fuel combustion results high material stresses and this is one of the challenges as well.

Post-combustion process of CO_2 removal is mostly applied in petrochemical, refining and gas-processing industries [5]. Post-combustion is the most mature technology in comparison to pre-combustion and oxy-fuel combustion. The advantage of post-combustion as end-of-pipe technology is that it can be implemented after the combustion process.

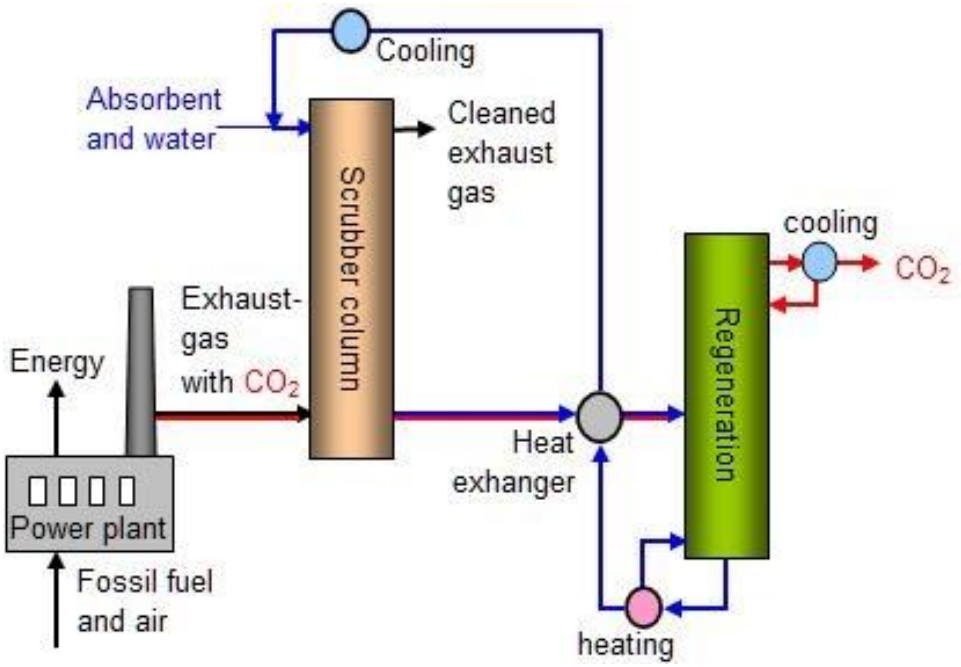

Figure 1-3: Post combustion CO_2 capture [6].

The principle of the process is that rich with CO_2 gas reacts with absorbent in absorption column also known as scrubber column. After the absorption column lean exhaust gas is released to atmosphere and rich with CO_2 absorbent gets into the regeneration column. In the regeneration column, CO_2 is separated from the absorbent, and CO_2 lean solution is directed back to the scrubber column. Operating temperatures in the absorption column are in the range 40-65 ^{o}C, in the regeneration column is near 100-150 ^{o}C. The temperature difference is the driving force between the absorption column and regeneration column.

Different technology options to separate CO_2 from the flue gas are represented on the Figure 1-4.

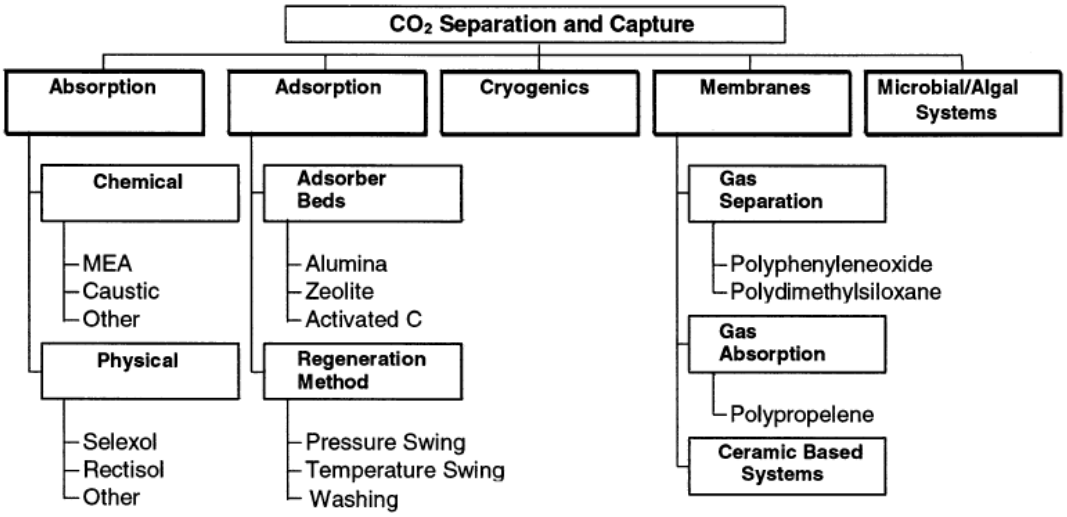

Figure 1-4: Technology options for CO_2 separation and capture [7].

This work is focused on the investigation of absorbents for chemical absorption process of CO_2 separation and capture.

1.3 Absorbents overview

1.3.1 Alkanolamine family

In order to choose the right absorbent, composition of the exhaust gas and its temperature and pressure conditions have to be taken into account [8].

Solvents are usually characterized by the next criteria [9]:

- reactivity with CO_2;
- regeneration costs;
- absorption capacity;
- solvent degradation;
- environmental impact;
- solvent cost.

Solvents from alkanolamine family are used in chemical CO_2 removal process. There are four main groups of alkanolamines: primary, secondary, tertiary amines and hindered amines.

Primary and secondary amines have two and respectively one hydrogen atoms attached to the nitrogen atom. Monoethanolamine (MEA), 2-(2-aminoethoxy) and Diglycolamine (DGA) are representatives of primary amines. Diethanolamine (DEA) and Diisoprapanolamine (DIPA)

belong to secondary amines. Tertiary amines do not have hydrogen atom attached to a nitrogen atom. Triethanolamine (TEA) and Methyldiethanolamine (MDEA) represent tertiary amines [8].

Reactions (1-1) – (1-4) represent the CO_2 absorption by primary/secondary amines with the modification of amines formula. Tertiary amines undergo all the reaction with the exception of carbamate formation reaction (1-4) [8] .

1. Ionization of water:

$$H_2 0 = H^+ + OH^- \quad (1\text{-}1)$$

2. Hydrolysis and ionization of dissolved CO_2:

$$CO_2 + H_2O = HCO_3^- + H^+ \quad (1\text{-}2)$$

3. Protonation of alkanoamine:

$$RNH_2 + H^+ = RNH_3^+ \quad (1\text{-}3)$$

4. Carbamate formation:

$$RNH_2 + CO_2 = RNHCOO^- + H^+ \quad (1\text{-}4)$$

Primary and secondary amines possess high absorption rate because they can react directly with the CO_2 through the carbamate reaction. Tertiary amines do not form carbamate, thus their absorption rate is significantly lower [5]. Because of high stability of the carbamate, the absorption capacity of primary amines is limited to 0.5 mole of CO_2 per mole of amine, while with tertiary amines 1 mole of CO_2 per mole of amine can theoretically be achieved [8].

A sterically hindered amines, is a group of amines with lower regeneration costs in comparison to primary or secondary amines [10]. This group can be defined as primary amine with the amino group attached to a tertiary carbon atom or a secondary amine with the amino group attached to a secondary or tertiary carbon atom [11]. 2-Amino-2-methyl-1-propanol (AMP) and 2-piperidineethanol (PE) represent primary and secondary sterically hindered amines respectively. The disadvantage of this group is a high material cost for commercial use [8].

1.3.2 Monoethanolamine

MEA solution is a proven chemical absorption technology. MEA has been commonly used as a solvent for CO_2 capture for many years. The advantages of MEA over other solvents are its high alkalinity, high reactivity and comparatively low cost.

Although presently other solutions replace MEA for the CO_2 capture in high pressure gas streams, MEA is still actual absorbent in systems with low concentrations of CO_2, were gas has to be treated at low pressures and maximum CO_2 removal is required [8].

High enthalpy of reaction of MEA with CO_2 requires high consumption of desorption energy. In the process of reaction with oxygen-bearing COS (carbonile sulfide) and CS_2 gasses, MEA is inclinable to form degradation products [12]. In order to avoid MEA degradation, SO_2 and NO_2 gasses have to be considerably reduced before the chemical absorption process. MEA with concentrations more than 30% is highly corrosive and its performance requires the usage of corrosion inhibitors [8]. Also one of the problems associated with MEA usage is high costs of regeneration process.

Regarding listed above disadvantages of MEA absorbent, development of new solvent systems with higher CO_2 characteristics become essential task.

1.3.3 Relationship between structure of amines and CO_2 absorption capacity

Alternatives to existing CO_2 capture absorbents can be found and designed with detailed study of the influence of amine structure on amine CO_2 capture capacity. Modification of amine structure can potentially eliminate disadvantages of currently used amines properties [13].

An expression “the change of amine structure” is quite wide and covers issues listed below [11, 14-19]:

- the introduction of substituent at α carbon;

In organic chemistry, α and β carbons refer to the position (first and second respectively) of the carbon that is attached to the functional group.

- the variation of the chain length;
- the variation of the number of functional groups;
- performance of side chain at the α -carbon position.

Amines represented in the Table 1- 1 were chosen for investigation in this work.

Table 1-1: Alkanolamine-based absorbents investigated in this work.

Amine	Chain
Monoethanolamine Formula :C_2H_7NO Molecular Weight : 61.08 g/mol	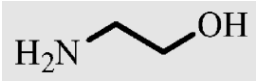
3-Amino-1-propanol Formula : C_3H_9NO Molecular Weight : 75.11 g/mol	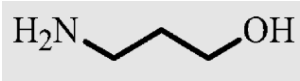
4-Amino-1-butanol Formula : $C_4H_{11}NO$ Molecular Weight : 89.14 g/mol	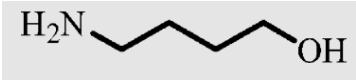
5-amino-1-pentanol Formula : $C_5H_{13}NO$ Molecular Weight : 103.16 g/mol	

Such factors as amine structure, process techniques, and conditions of the reactions complicate the impact of structural change on the amines CO_2 absorption capacity [13]. Thus, better insight in the problem of influence of amine structures on their abilities in CO_2 capture is important to achieve higher efficiencies of CO_2 absorbents.

Literature research regarding the influence of amine chemical structure on its ability to absorb CO_2 and the results of VLE experiments to represent this effect were performed in this thesis.

1.4 Outline of the thesis

This Thesis aims to investigate the effect of the chain length between the amine and hydroxyl group and substitution on α -carbon on the CO_2 absorption ability of different alkanolamines. Selected amines have different chain length: from two - carbon chain in MEA to five - carbon chain in 5-amino-1-pentanol (5A1P). MEA was chosen as a base case since it is considered as

proven technology for CO_2 capture process [20] and numerous data of equilibrium measurements are available in literature [21-28]. For a fair comparison, concentrations of all investigated aqueous amine solutions were kept at 30(wt)%. The temperature during the experiments was maintained 40°C, and CO_2 loading in the range 0.2-0.5. The specified experimental conditions were chosen to cover the range of operating conditions for chemical absorption process in power plants. The 5-amino-1-pentanol (5A1P), 4-amino-1-butanol (4A1B) and 3-amino-1-propanol (MPA) amines may be useful for CO_2 capture technology and haven't been investigated enough. The CO_2 solubility data of these aqueous amine solutions will be used to provide data for thermodynamic modeling in the near future.

In this work, experiments were run using equilibrium cell equipment. Equilibrium CO_2 partial pressures were measured using gas chromatograph (GC) set-up and CO_2 loadings were analyzed with $BaCl_2$ titration method [29-32].

Chapter 1 introduces a holistic overview of CO_2 capture issues with determination of the task and description of the performed work in this thesis.

Literature review of research articles about VLE in amine-water- CO_2 systems, specifically primery amines MEA, MPA, 4A1B and 5A1P is represented in Chapter 2. Also Chapter gives introduction to the influence of structural change of amines on their CO_2 capture activities.

Chapter 3 presents VLE measurements of CO_2 equilibrium partial pressures, CO_2 loadings and amines concentrations. Detailed description of equilibrium cell set – up and titration equipment design, experiment procedures are performed in chapter 3 as well.

Chapter 4 discusses comprehensively calculations of measurement uncertainty. The uncertainty analyses were performed for MPA, 4A1B and 5A1P. Only one sample calculation will be discussed in details since the calculation procedure is the same for each amine.

Results of the measurements and discussion are presented in chapter 5.

Chapter 7 gives suggestions for further work.

2 Literature research

2.1 Previous vapor-liquid- equilibrium studies of amine-water- CO_2 systems

2.1.1 Monoethanolamine

Reactions between the aqueous MEA solution and CO_2 can be represented with the equations (1-1)-(1-4) in Chapter 1.

The VLE measurement literature data for CO_2 solubility in a 30 mass% MEA at 40 ºC temperatures is represented in Table 2-1.

Table 2-1: Literature review of 30 (wt) % MEA.

Year	Author	Pressure range, kPa
1995	Jou et al. [21]	0.001 - 19914
2012	Tong et al.[22]	3.95-161.52
2011	Aronu et al.[23]	0.0016 - 11812
1974	Lee et al. [24]	2.805 - 5973.214
1976	Lee et al. [25]	0.1 - 10000
1992	Shen et al.[26]	2.2 – 1973
2013	Jayarathna et al.[28]	0.0099-15.593

The comparison of data is represented in details in Chapter 4.

2.1.2 5-amino-1-pentanol, 4-amino-1-butanol and 3-amino -1-pentanol

Primary amines 5A1P, 4A1B and 3A1P are new potential CO_2 absorbents. The process of CO_2 absorption was investigated in detail only for 3-amino-1-pentanol.

The process of CO_2 absorption in MPA at high partial pressures aqueous solution was analyzed by Camacho et al. in [33]. As can be observed in the results published in this work, the increase of initial concentration leads the increase in the volumetric flow of absorbed CO_2.

The reactions of MPA with CO_2 for CO_2 loadings $\alpha < 0.5$ are represented with equation 2-1 and equation 2-2 [33]:

$$RNH_2 + CO_2 \rightarrow RNHCOO^- + H^+ \qquad (2\text{-}1)$$

$$RNH_2 + H^+ \rightarrow R^-NH_3^+ \qquad (2\text{-}2)$$

According to [33], for CO_2 loadings $\alpha < 0.5$, there are three possible reaction mechanisms:

1) Hydrodynamic regime or physical absorption, takes place when $C_{Bo}/2C_A^* \ll 1$ with absorption rate represented with the equation 2-3:

$$N_A = k_L \cdot C_A^* \qquad (2\text{-}3)$$

2) Instantaneous-reaction regime when $1 \ll C_{Bo}/2C_A^* \ll \sqrt{kC_{Bo}\,\theta}$:

$$N_A = k_L \frac{C_{Bo}}{2} \qquad (2\text{-}4)$$

3) Fast-reaction regime occurs when $\sqrt{kC_{Bo}\,\theta} \ll C_{Bo}/2C_A^*$:

$$N_A = C_A^* \sqrt{kC_{Bo}\,D_A} \qquad (2\text{-}5)$$

Where:

N_A - rate of absorption per unit interfacial area, $kmol/m^2s$;

C_{Bo} - initial concentration of amine in aqueous phase, $kmol \cdot m^{-3}$;

C_A^* - CO_2 concentration in equilibrium with gaseous phase, $kmol \cdot m^{-3}$;

k - reaction rate constant;

k_L - liquid-phase mass-transfer coefficient, $m \cdot s^{-1}$;

D_A – diffusion coefficient of component $A(CO_2)$ in aqueous alkanolamine solution, $m^2 \cdot s^{-1}$;

θ – average life of surface elements, s.

For CO_2 loadings $\alpha > 0.5$, additional reaction takes place:

$$RNHCOO^- + 2H_2O + CO_2 \rightarrow R^-NH_3^+ + 2HCO_3^- \quad (2\text{-}6)$$

The solubility of CO_2 in MPA aqueous solutions was investigated by Dong et al [34]. The data of VLE measurements of CO_2 partial pressures in 2 $mol \cdot dm^{-3}$ and 4 $mol \cdot dm^{-3}$ MPA aqueous solutions at 40 °C temperature is represented in the Table 2-2 and Table 2-3 respectively.

Table 2-2: Solubility of CO_2 in 2 mol·dm-3 MPA aqueous solutions at 40 °C temperature [34].

α, mol CO_2/mol MPA	P_{CO_2}, kPa
0.566±0.05	4.5±0.5
0.669±0.05	20.6±0.5
0.731±0.06	45.1±1
0.805±0.06	100.7±2
0.849±0.07	153.9±3
0.876±0.07	202.0±4
0.947±0.08	377.6±8
0.987±0.08	525.6±11
1.024±0.08	695.0±14

Table 2-3: Solubility of CO_2 in 4 mol·dm-3 MPA aqueous solutions at 40 °C temperature [34].

α, mol CO_2/mol MPA	P_{CO2}, kPa
0.527±0.04	7.8±0.5
0.58±0.05	18.2±0.5
0.675±0.05	76.5±2
0.752±0.06	191.2±4
0.793±0.06	293.5±6
0.828±0.07	414.8±8
0.856±0.07	548.6±11
0.876±0.07	654.8±13

Kinetics of carbon dioxide with 3-amino-1-propanol aqueous and non-aqueous solution was investigated by Kadiwala et al. [35].

There is no available literature data regarding solubility of CO_2 in 5-amino-1-pentanol and 4-amino-1-butanol aqueous solutions. However, in a number of publications, discussed in Chapter 2.2, MEA, MPA, 4A1B and 5A1P are compared by their structural difference with respect to CO_2 capture activities.

2.2 Influence of structural change of amines on their CO_2 capture activities

A number of investigators have studied structure-activity relationships for hindered amines.

In [11], Sartori and Savage revealed α –substituent positive effect for high CO_2 loadings. The same effect was described in Chakraborty et al. publication [17] and explained with carbamate instability created by α -carbon, which caused the high CO_2 loadings.

Hook's publication [18] represented the dependence of amine structures on CO_2 loading in absorption and desorption. The increase of CO_2 loading and the decrease in absorption rate was observed with the change of amine structures from MEA to AMP.

Yang et al. [13] investigated primary amines with carbon chain length from 2 to 6 and concluded that carbon chain length doesn't influence considerably to CO_2 capture capacities of this group of amines.

Singh et al. investigations in the effect of the structure and molecular weight of amines, particularly MEA, 3-amino-1-propanol, 4-amino-1-butanol and 5-amino-1-pentanol on CO_2 absorption capacity are represented in [14],[16], [15] and [19] publications.

Results published in [14] showed that absorption capacity, in mol of CO_2 per kg of amine, will slightly increase with the increase of the chain length. However, the absorption rate and the absorption capacity, in mol of CO_2 per mol of amine, decreased with the same increase of the chain length.

The desorption capacity of MEA, 3-amino-1-propanol, 4-amino-1-butanol and 5-amino-1-pentanol is represented in [16]. The increase in desorption rate was observed with the increase of the carbon chain length from 2 (MEA) to 4 (4-amino-1-butanol), however further increase in the chain length led to decrease of the initial desorption rate.

Further Singh et al. studies published in [15], showed the effect of the position of substituted hydroxyl groups on CO_2 absorption capacity. As the result was the increase in CO_2 absorption capacity with substitution of hydroxyl group at α-carbon, known as steric hindrance effect, earlier described in [11], [17] and [18].

CO_2 solubility in 5-amino-1-pentanol was studied by Singh et al. [19]. The results of the work are represented on the Figure 2-1.

Cyclic capacity, represented in Figure 2-1, is the difference of concentrations at absorption and stripping processes, and can be defined with equation 2-10 [36]:

$$Q = C_{amine}\,(\alpha - \alpha_{lean}) \qquad (2\text{-}10)$$

Where:

C_{amine} - amine concentration;

α – rich CO_2 loading;

α_{lean} - lean CO_2 loading

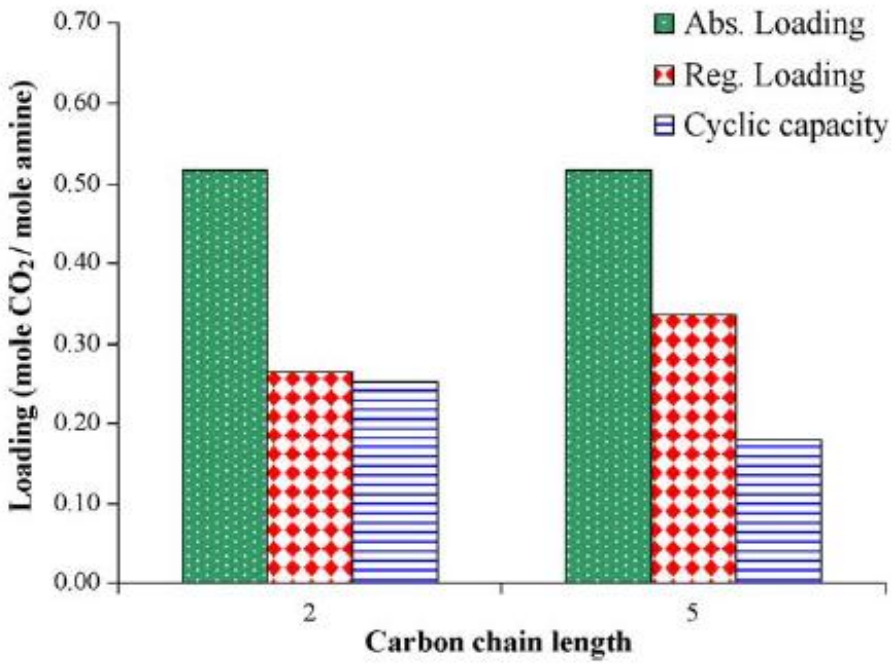

Figure 2-1: Effect of chain length in alkanolamine-based solvents for 2.5 mole/L concentration [19].

In the Figure 2-1, where the CO_2 loading, mole CO_2/mol amine, in MEA (carbon chain length=2) is compared to CO_2 loading in 5-amino-1-pentanol (carbon chain length=5). Higher carbon chain results higher lean loading without any change in rich loading. This is the reason for lower net cyclic capacity in 5-amino-1-pentanol comparably to MEA.

3 Solubility of CO_2 in alkanolamines

3.1 Introduction

The CO_2 partial pressures and CO_2 loadings in MEA, MPA, 4A1B and 5A1P under the same equilibrium conditions were investigated in this work. The experiments were run at atmospheric pressure and 40°C temperature. The concentration of chosen aqueous amines is 30wt%, the range of CO_2 loadings is 0.2-0.55 mole CO_2 /mole amine. VLE curve of 30% aqueous MEA was chosen as a base case because of possibility to compare it with the MEA VLE curve obtained by Jayarathna et al. [28] using the same experiment equipment at the relevant equilibrium conditions.

Aqueous amine solutions were loaded with CO_2 in equilibrium cell with constant temperature during the experiment. The partial pressure of CO_2 in the gas phase was examined with gas chromatograph. The CO_2 loading in a liquid phase was analyzed with $BaCl_2$ titration method.

3.1.1 Gas chromatography

Gas chromatograph (GC) is an instrument, used for measuring the content of components in sample. The analytic technique, used in gas chromatograph is gas chromatography. Chromatography is an analytic technique of mixture separation.

The main elements of GC are:

- injection port;
- separation column;
- mobile phase that dissolves and carries the sample mixture;
- stationary phase in separation column;
- detector;
- recording system.

The GC is schematically represented on the Figure 3-1.

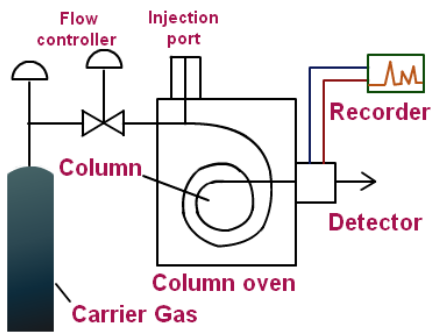

Figure 3-1: Schematic of a gas chromatograph [37].

In gas chromatography gas is used as mobile phase. The sample is injected through injection port in GC and with gas stream is transported to separation column. The quantity of the components is measured with detector. The standard sample with known concentration is injected to the instrument in order to determine the concentration of the tested sample. The concentration is calculated by the comparison of the peak retention time of the standard and test samples. Retention time – is a time for compound to reach the detector through the column.

3.1.2 Titration

Titration, known as volumetric analysis, is method used in quantitative chemistry to determine the concentration of investigated substance. Investigated substance is also called titrand or analyte while the reagent is known as titrant. The type of the reaction between the titrant and titrand determine the type of titration. There are three types of titrations commonly used in inorganic chemistry: asid-base, redox and complexometric. In this work acid-base titrations are performed. A back titration, known as reverse titration, is used to titrate the reactant with known concentration.

The type of asid-base titration depends on the strength of the reactants:

- strong acid with a strong base;
- strong acid and weak base;
- weak acid and strong base;
- weak acid and weak base.

Titration curve represents the relationship between pH and added titrant, as is shown on the Figure 3-2.

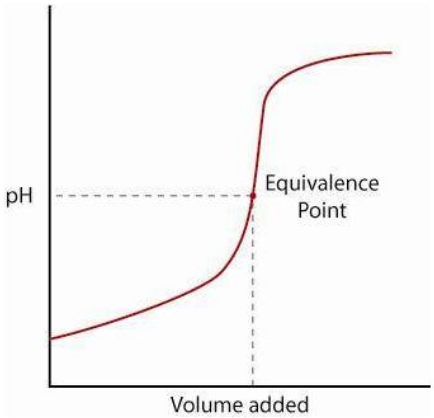

Figure 3-2: Strong acid titration curve [38].

The point on the titration curve where the volume of added titrant is enough for complete neutralization of the solution is called equivalence point [38].

The end point of titration is the completion of the titration indicated with some physical change of the titrant.[38].

3.2 Materials

N_2 (purity 99.99 %) and CO_2 (purity 99.99%) gasses were supplied by Yara Praxair AS. Aga Gas supplied CO_2 gas of concentrations 15%, 7%, 0.98% and 0.085% for GS calibration. Sample solutions of amines were prepared mixing the received chemicals with degassed water. Monoethanolamine (MEA) - $[H_2N(CH_2)_2OH]$ of more than 99.5% purity was obtained from Merck KGaA, Germany. 3-Amino-1-pentanol (MPA) – $[HO(CH_2)_3NH_2]$ of 99% purity, 4-amino-1-butanol - $[H_2N(CH_2)_4OH]$ of 98% purity and 5-amino-1-pentanol – $[NH_2(CH_2)_5OH]$ (purity 95%) were obtained from Sigma-Aldrich Norway AS.

Sodium hydroxide (NaOH) of 0.1M concentration and hydrochloric acid (HCl) of 0.1 and 1 M concentration for $BaCl_2$ titration were prepared from the chemicals from MERCK in mixtures with deionized water. Buffer solutions of pH 4.01, 7 and 9.21 where purchased from Mittler Toledo for DG 300-SC electrode calibration.

3.3 Equilibrium cell apparatus design

Schematic diagram of equilibrium cell represented in the Figure 3-3. The purpose of equilibrium cell is to obtain specified pressure and temperature in the vapor and liquid phase of the investigated amine. The equilibrium cell was designed by Tel-Tek organization on the

principles of low VLE apparatus for atmospheric pressure described in works [36] , [39] and [23]. The VLE apparatus was proven to give highly accurate data in [28] where the measurement results for 30% MEA at 40 ℃ were represented and compared with literature data for MEA at the same VLE conditions.

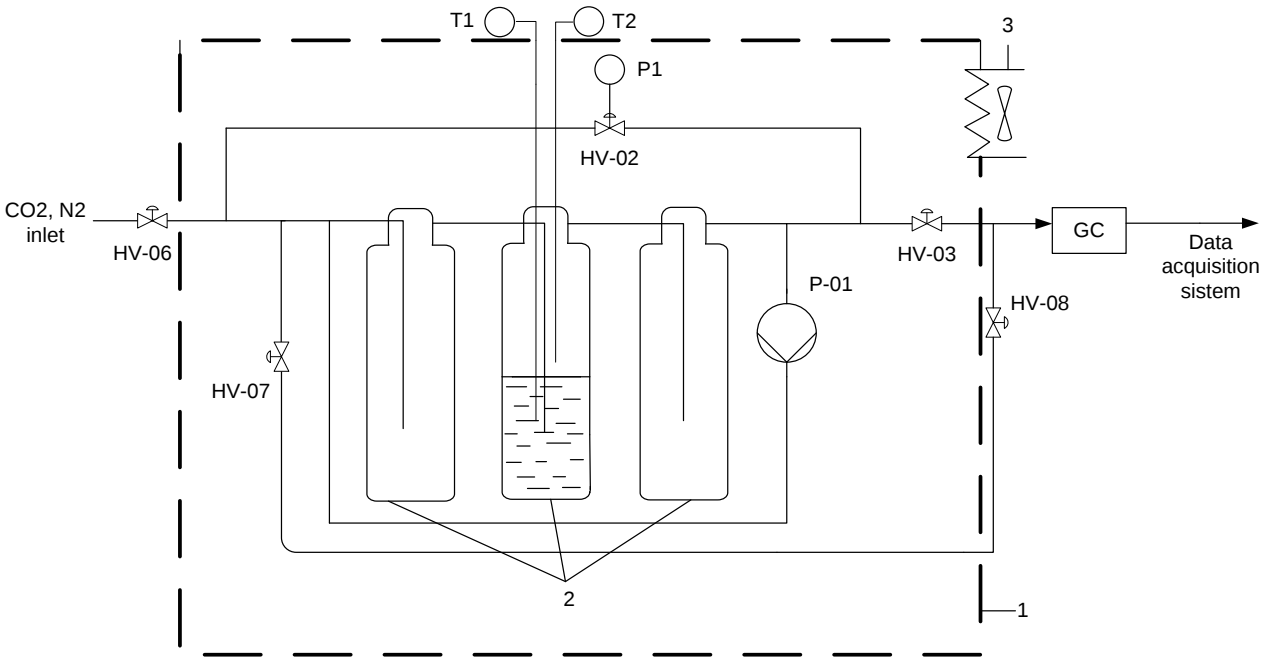

Figure 3-3: Schematic diagram of Equilibrium cell set-up.

T1, T2 – thermocouples, P1- pressure measurement , P-01 – pump, GC-gas chromatograph, 1- isolated box, 2-glass flasks, 3- heating fan, HV-02-HV-08– valves, used in the equilibrium cell.

The specification of the apparatus equipment and the purpose of each valve on the schematic diagram are presented in the Table 3-1 and Table 3-2 respectively.

The main systems of equilibrium cell apparatus are:

1) Equilibrium cell
2) Gas supply system
3) Temperature control system
4) Gas chromatograph
5) Data acquisition system

As can be seen from Figure 3-3 and Figure 3-4 c), equilibrium cell is performed as isothermal box with heater and pump, where CO_2 gas is circulated by rubber tubes through aqueous amine solution. The set-up includes three glass flasks while the amine solution is contained in the second glass flask. Two glass flasks on each side of the flask with amine solution serve to

avoid the pressure drop when the samples are extracted and to prevent liquid leakage into the system.

a *b* *c*

Figure 3-4: Equilibrium cell apparatus.

Figures 3-4 represent a) valves for CO_2 and N_2 gases, b) gas flow controllers (Sierra), c)Equilibrium cell.

The set-up is designed to run the experiment in closed system with constant temperature and atmospheric pressure. The N_2 and CO_2 gas system is connected with the equilibrium cell by valves HV 664 and HV 158, shown in the top of the Figure 3-4 a). The bottom of the Figure 3-4 a) shows inlets and valves for calibration gases. The gas flow rate is controlled with the Sierra flow meters, represented in the Figure 3-4 b).

The temperature control panel, shown in the top of the Figure 3-4 a) and b) is set to maintain the specified temperature for VLE conditions. Temperatures in the solution and the environment are collected through thermocouples with temperature logger and visualized on the computer monitor, shown in the Figure 3-5 c). Thermocouples are defined as T1 and T2 on the schematic diagram in the Figure 3-3. The pressure limit for the set up during the experiment is 0.35 mbar. Pressure is monitored with the pressure gauge, represented in the bottom of Figure 3-4 a) and b).

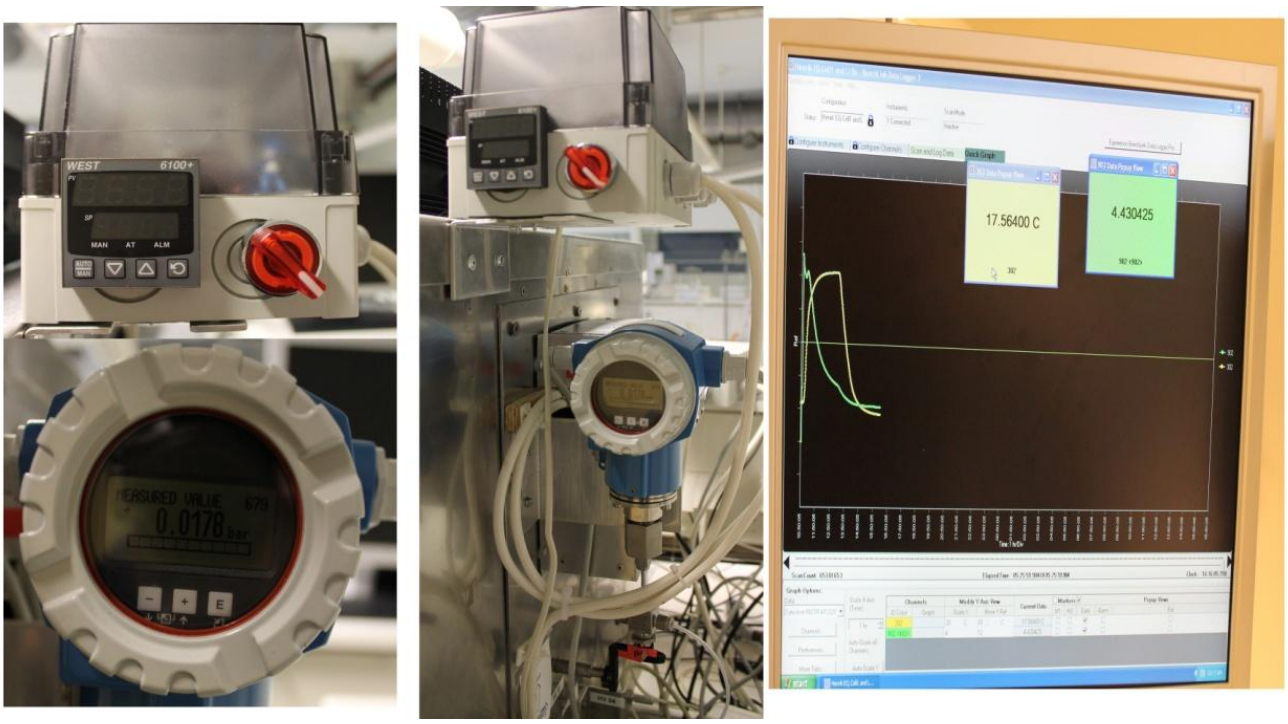

a b c

Figure 3-5: Elements of equilibrium cell apparatus.

Figures 3-5 represent a) *top* Temperature controller, a) *bottom* Pressure gauge b) temperature controller and pressure gauge connected to equilibrium cell c) PC monitor.

Table 3-1: Elements of the equilibrium cell.

Element	Material	Number of units	Specification	Purpose	Manufacturer	Model
1	2	3	4	5	6	7
Flask	glass	1	250 cm^3	Load MEA solution with CO_2		
Flask	glass	2	500 cm^3	Avoid solution penetration in to the system		
Tubes	silicon			Connection for the flasks		

Table 3-1 (Continued).

1	2	3	4	5	6	7
Gas chromatographer				Analysis of the gas phase	Thermo-Scientific	KAV00349
Pump	P-01, DC	1	130 l/h	Circulation of the CO_2 through the sample	Hardi	18812
Heater		1		Maintain specified temperature in the system		
Pressure gauge		1		Pressure readings	Endress & Hauser	Cerabar S
Flow meter		1		CO_2 flow rate readings		
Flow controller	FIC 158	1		Control N_2 flow rate		Sierra
Flow controller	FIC 670	1		Control CO_2 flow rate		Sierra
Temperature control panel		1		Set required temperature	West 6100	West instruments-Process controls
Temperature logger		1		Visualization and log of the temperature data		
Thermo-couple		2	Type K	Temperature measurement		

Table 3-2: Valves used in the equilibrium cell system.

Valve number	Purpose
HV- 02	Pressure control
HV-03	Flush the system
HV-04	Flush the system with calibration gas
HV-06	Connection of the EQ-cell with the laboratory gas system
HV-08	Shift the gas sample to GC
HV-158	N_2 supply to EQ-cell
HV-670	CO_2 supply to EQ-cell

3.4 Measurement of CO_2 partial pressure in the gas phase

30 wt% aqueous amine solution was prepared by diluting amine with degassed water. Degassed water was prepared using rotavapor BUCHI R-210 and vacuum pump BUCHI V-710 shown in the Figure 3-6 a). All gravimetric measurements were done with Mettler XS-403S precision balance represented in the Figure 3-6 b).

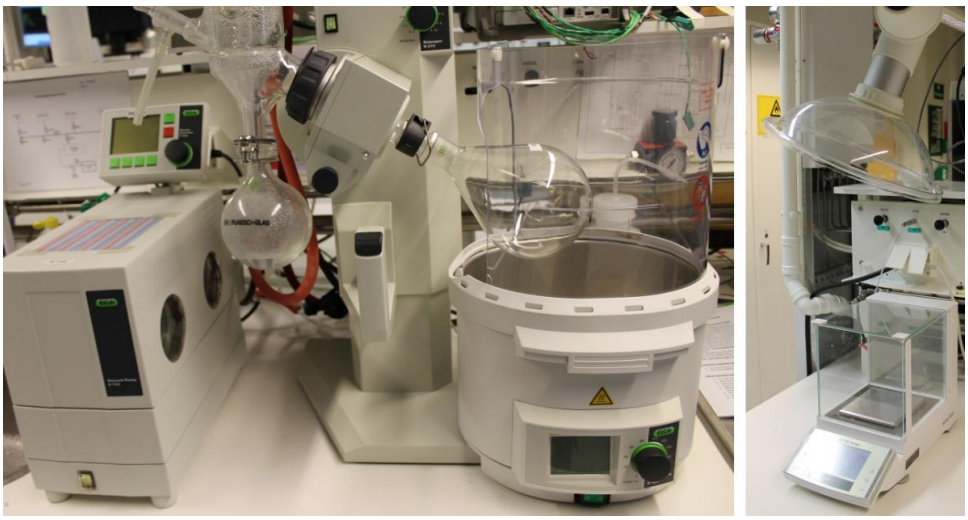

a b

Figure 3-6: Laboratory equipment.

Figures 3-6 represent a) rotavapor, b) Precision balance

The experiments were run following the procedure precisely described in [27] from the desorbtion side. This means that solution was firstly loaded with CO2 to some specified level, what was further decreased.

Firstly, before adding amine solution in the flask, system was checked on the leakage by pressurizing it with N_2 till the pressure value on the pressure gauge reached 0.35 mbar.

If the pressure value on the pressure gauge was stable during several minutes, the system was depressurized and filled with amine solution. After the equilibrium cell was flashed with CO_2 and all the other gasses were removed from the system, the amine solution was loaded with CO_2 in the equilibrium cell during time corresponding to the specified loading. Loading time was calculated with the equations:

$$\alpha = \frac{n_{amine}}{n_{CO_2}} \tag{3-1}$$

$$n_{CO_2} = \alpha \cdot n_{amine} \tag{3-2}$$

$$n_{amine} = \frac{m_{amine}}{M_{amine}} \tag{3-3}$$

$$m_{amine} = [m_{amine\ total} - m_{amine\ remaining}] \cdot \frac{x}{100} \tag{3-4}$$

$$PV_{CO_2} = n_{CO_2}RT \tag{3-5}$$

$$V_{CO_2} = \frac{n_{CO_2}RT}{P} \tag{3-6}$$

$$t_{loading} = V_{CO_2}/\dot{V}_{CO_2} \tag{3-7}$$

Where:

x-number of measurement;

α – CO_2 loading mol CO_2/ mol amine;

n_{CO_2} – number of CO_2 moles;

n_{amine} – number of amine moles;

P - pressure, kPa;

T – temperature, °C;

R – gas constant, $\frac{J}{K \cdot mol}$;

m_{amine} - mass of amine, g

M_{amine} - molar mass of amine, g/mol;

V_{CO_2} - volume of CO_2, m^3;

$\dot{V}_{CO_2}$ – volumetric flow of CO_2, m^3/s.

After amine was loaded with CO_2, the system was flushed during 5 minutes with N_2 in order to drive out dissolved in the solution O_2. Afterwards the temperature set point was set to 40°C. N_2 and CO_2 gas mixture was circulated for 1 hour after the temperature in gas and liquid phases stabilized to 40°C . During the experiment, the temperature was controlled with computer monitor, shown on the Figure 3-5 c).

Afterwards the system obtained VLE conditions gas sample was extracted to GC, represented on the Figure 3-3 and Figure 3-7.

Figure 3-7: Gas chromatograph.

The GC was calibrated with certified calibration gases. The choice of calibration gas depended on the concentration of CO_2 in the sample. The samples were extracted from the closed loop to GC, where the gas CO_2 content of the samples was analyzed and the data was collected with Chromeleon software. Partial pressure data is represented in Appendix 2, Appendix 3, Appendix 4 and Appendix 5.

3.5 Measurement of CO_2 loading and amine concentration in the liquid phase

The liquid sample was extracted from the equilibrium cell after the gas phase was analyzed in GC.

CO_2 loading of amine and its concentration was measured with $BaCl_2$ precipitation – titration method using Titrator Mettler Toledo T50, shown on the Figure 3-8 and following procedures [29-31]. The method is also described in [32].

Figure 3-8: Titrator Mettler Toledo T50.

3.5.1 CO_2 loading measurement

50 cm^3 of 0.1 mol sodium hydroxide (NaOH) was added in 250 cm^3 Erlenmeyer flask (EM). Correspondingly to the amine concentration and the CO_2 loading in the sample, the exact amount of liquid sample in the range of 0.3 - 0.5 g was added afterwards. The added mass of CO_2 highly loaded samples should be lower the mass of less loaded samples. Then 50 cm^3 of 0.3 M barium chloride $BaCl_2$ was added to the same flask. EM flask was closed with the rubber stopper and put on a heater at 270 °C. The Erlenmeyer flask was heated until the formation of barium carbonate $BaCO_3$. After 5 minutes of boiling, the mixture was cooled to the ambient temperature in the water bath and filtered. Filtrate was gathered on the filter paper, put to the 250 ml beaker with magnet stirrer and poured over with 100 ml of degassed water.

$BaCO_3$ was titrated with 0.1M HCl to pH2, till all $BaCO_3$ precipitate was dissolved and CO_2 released. The volume of consumed 0.1M HCl was noted.

Afterwards the mixture was again boiled on the heater at 270 °C temperature and cooled in the water bath to the ambient temperature. The mixture was back-titrated with 0.1 M NaOH till the equivalence point at pH7, as is shown in the Figure 3-9. The volume of consumed 0.1M NaOH was noted.

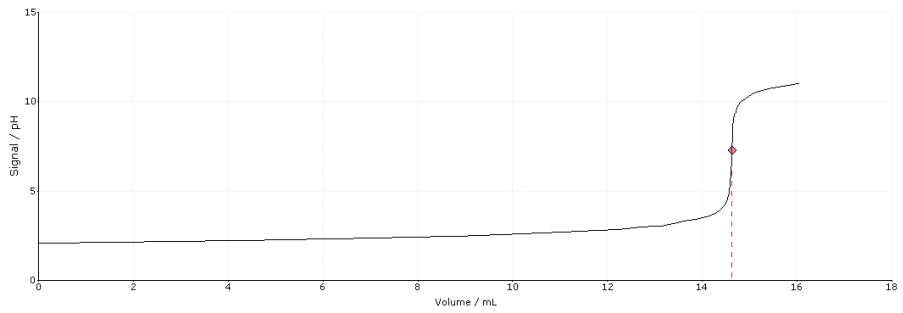

Figure 3-9: Titration with 0.1M NaOH.

Reactions corresponding to $BaCl_2$ titration can be represented with equations (3-8)-(3-10) [30]:

Barium carbonate formation:

$$Ba^{2+} + CO_2 + 2OH^- \rightarrow BaCO_3 + H_2O \quad (3\text{-}8)$$

Titration with 0.1M hydrochloric acid:

$$BaCO_3 + 2HCl \rightarrow BaCl_2 + CO_2 + H_2O \quad (3\text{-}9)$$

Back-titration with 0.1M sodium hydroxide:

$$HCl + NaOH \rightarrow NaCl + H_2 \quad (3\text{-}10)$$

3.5.2 CO_2 concentration measurement

Exact mass of the liquid sample in the range from 1 to 2 g was added to 250 ml beaker. The mass of added sample was recorded. 100 ml of distilled water was added to the beaker. The solution was titrated with 1M HCl to equivalence point as is shown on the Figure 3-10.

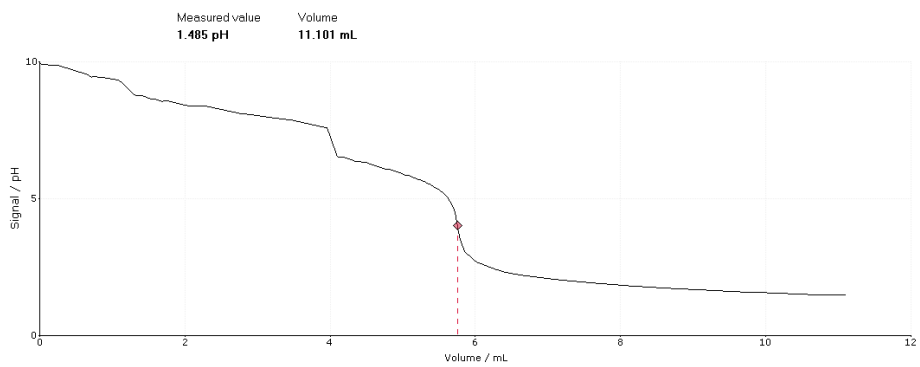

Figure 3-10: Titration with 1M HCl.

The value of consumed volume of HCl was noted. The reactions of HCl titration can be represented with equations (3-11)-(3-12):

$$NH_2CH_22OH + H_2O \rightarrow H_3N(CH_2)_2OH + OH^- \quad (3\text{-}11)$$

$$OH^- + HCl \rightarrow H_2O + Cl^- \quad (3\text{-}12)$$

3.5.3 CO_2 loading and amine concentration calculation

The CO_2 loading of amine and amine concentration can be calculated with the equations (3-13) - (3-20)

The amount of CO_2 moles in the sample and the blank sample:

$$n_{CO_2\ \text{in sample}} = \frac{C_{HCl} \cdot V_{HCl} - C_{NaOH} \cdot V_{NaOH}}{2} \quad (3\text{-}13)$$

$$n_{CO_2\ \text{in BS}} = \frac{C_{HCl} \cdot V_{HCl\ BS} - C_{NaOH} \cdot V_{NaOH\ BS}}{2} \quad (3\text{-}14)$$

The mass of CO_2 in the sample and the blank sample:

$$m_{CO_2\ \text{in BS}} = n_{CO_2\ \text{in BS}} \cdot M_{CO_2} \quad (3\text{-}15)$$

$$m_{CO_2\ \text{in sample}} = n_{CO_2\ \text{in sample}} \cdot M_{CO_2} - m_{CO_2\ \text{in BS}} \quad (3\text{-}16)$$

The mass of amine solution in the sample:

$$m_{MEA+water} = m_{\text{sample loading}} - m_{CO_2\ \text{in sample}} \quad (3\text{-}17)$$

$$\frac{n_{CO_2}}{m_{MEA+water}} = \frac{n_{CO_2\ \text{in sample}} - n_{CO_2\ \text{in BS}}}{m_{MEA+water}} \cdot 100 \frac{g}{kg} \quad (3\text{-}18)$$

$$f = \frac{m_{CO_2\ \text{in sample}}}{m_{\text{sample ,loading}}} \quad (3\text{-}19)$$

Mass of amine:

$$m_{MEA,conc} = C_{HCl} \cdot V_{HCl} \cdot M_{MEA} \tag{3-20}$$

$$m_{(MEA+water),conc} = m_{sample,conc} - m_{CO_2} = m_{sample,conc} - f \cdot m_{sample,conc} \tag{3-21}$$

Concentration of aqueous amine:

$$wt\%MEA = \frac{m_{MEA,conc}}{m_{(MEA+water),conc}} \tag{3-22}$$

CO_2 loading:

$$\frac{n_{MEA,conc}}{m_{(MEA+water),conc}} = \frac{\frac{wt\%MEA}{100\%}}{M_{MEA}} \cdot 1000 \frac{g}{kg} \tag{3-23}$$

$$\alpha = \frac{\frac{n_{CO_2}}{m_{MEA+water}}}{\frac{n_{MEA,conc}}{m_{(MEA+water),conc}}} \tag{3-24}$$

Calculated CO_2 loadings are represented MEA, MPA, 4A1B and 5A1P concentrations are represented in Appendix 6, Appendix 7, Appendix 8 and Appendix 9.

4 Uncertainty analysis

4.1 Introduction

The indication of uncertainty is an important part of reporting experimental data. Without uncertainty analysis, measurement data are meaningless and cannot be compared with reference literature values.

In order to develop common approach for international comparison of measurement results, the Bureau International des Poids et Mesures (BIPM) organization published a report entitled – "Guide to the expression of uncertainty in measurement" or "GUM" in 1993 [40] with further corrections and reprint in 1995 [41] and in 2008 [42]. GUM is concerned with uncertainty expression for physical experiments.

In 1995, following "GUM", a standard document for uncertainty analyses called "Quantifying uncertainty in analytical measurement" also known as "QUAM", was published for analytical chemistry with a second edition in 2000 [43].

Measurement uncertainty is characteristic, used to determine authenticity of the measurement data[44]. The definition of measurement uncertainty according to "GUM": "Parameter, associated with the result of measurement, that characterizes the dispersion of the values that could reasonably be attributed to the measurand" [40]. Where measurand – is physical quantity, precisely defined and characterized by unique value [42].

In most of the cases, it is impossible to estimate directly the measurand value, thus it is calculated through other measured quantities. The functional relationship between the unknown measurand and measured quantities is represented with equation (4-1) and is called "measurement model" [42] .

$$Y = f(X_1, X_1, \dots, X_N) \qquad (4\text{-}1)$$

Where:

Y – measurand or output quantity;

X - measured or input quantity.

When measurand is estimated through measurement model, its uncertainty is obtained by propagation of input quantities uncertainties. Propagation – is mathematical combination of the uncertainties [42].

Uncertainties of input quantities are usually expressed in a form of standard deviations and are called standard uncertainties, $u(x_i)$.

The uncertainty of an output estimated by uncertainty propagation is called the combined standard uncertainty, $u_c(Y)$.

An expected uncertainty U, is obtained by multiplying the combined standard uncertainty with the coverage factor as shown in equation (4-2). The expected uncertainty is used to evaluate an interval from $Y - U$ to $Y + U$.

$$U = u_c(M) \cdot k \qquad (4\text{-}2)$$

Where k – is the coverage factor, with value in the range from 2 to 3. Coverage factor is defined according to required level of confidence.

The uncertainty analyses were performed following the procedure presented in [42, 43, 45].

Since the calculation procedures are the same for all samples studied, only one example is shown in the Sections 4.2 and 4.3 of this Chapter. The chosen sample is sample 1 of 30% wt MEA. The standard uncertainty calculations for CO_2 partial pressures and CO_2 loadings of studied samples are presented in Chapter 5.

Measured data from GC of CO_2 partial pressures and calculated standard deviations for MEA, MPA, 4A1B and 5A1P is represented in Appendix 2, Appendix 3, Appendix 4 and Appendix 5 respectively.

4.2 Uncertainty analysis for measured values of CO_2 partial pressure in gas samples

Main uncertainty sources for partial pressure of CO_2 in a gas sample are [28]:

- temperature measurement T;
- concentration of aqueous MEA solution C_{MEA} ;
- total pressure measurement P;
- peak area A in gas chromatograph.

Relationship between the partial pressure of CO_2 in a gas sample and listed parameters can be shown using equation (4-1).

$$p_{CO_{2_i}} = f(T, C_{MEA}, P, A)$$

Combined standard uncertainty of P_{CO_2} in a gas phase can be calculated with the equation (4-3) [44]:

$$u_c(Y) = \sqrt{\sum_{i=1}^{n} \left\{\frac{\partial Y}{\partial x_i}\right\}^2 u^2(x_i)} \qquad (4\text{-}3)$$

Where:

Y – analytical result, measurand;

x_i - uncertainty source;

$u(x_i)$ - standard deviation of uncertainty source.

According to [44], equation (4-3) can be simplified to equation (4-4):

$$\frac{u_c(Y)}{Y} = \sqrt{\sum_{i=1}^{n} \left(\frac{u(x_i)}{x_i}\right)^2} \qquad (4\text{-}4)$$

The extended form of the Equation (4-4) is represented with the equation (4-5).

$$\frac{u_c(p_{CO_{2_i}})}{p_{CO_{2_i}}} = \sqrt{\left(\left(\frac{u(C_{MEA})}{C_{MEA}}\right)^2 + \left(\frac{u(p)}{P}\right)^2 + \left(\frac{u(A)}{A}\right)^2 + \left(\frac{u(T)}{T}\right)^2\right)} \qquad (4\text{-}5)$$

The uncertainty of total pressure changes was neglected because the experiments were run at the pressure close to atmospheric.

$$u(p) \approx 0$$

Main uncertainty source for MEA concentration is a weight measurement [28]. For equilibrium measurements of 30% (wt) MEA at 40 ℃ the concentration uncertainty was calculated below 0.0008 mass% and was considered negligible [28].

$$u(C_{MEA}) \approx 0$$

Uncertainty of the temperature measurement is $u(T) = \pm 0.1^{o}C$ [28]. The experiment on the GC was running with the average temperature 40℃ .

Average value and standard deviation of CO_2 partial pressure are taken from the Appendix 2.

$$\frac{u_c(p_{CO_2})}{p_{CO_2}} = \sqrt{(0.005448)^2 + \left(\frac{0.1}{40}\right)^2} = 0.054 = 5.4\%$$

Combined uncertainty for CO_2 partial pressure was calculated:

$$u_c(p_{CO_2}) = p_{CO_2} \cdot 0.054 = 31.962 \cdot 0.054 = 1.743 \text{ kPa}$$

Expanded uncertainty $U(p_{CO_{2_i}})$ was calculated using the equation (4-2). The value of the coverage factor k for the confidence interval 95% equals 2 [46].

Thus,

$$U(p_{CO_2}) = 0.097 \cdot 2 = 3.486 \text{ kPa}$$

Calculated uncertainties of CO_2 partial pressures for each sample are represented in chapter 4.

4.3 Uncertainty analysis for values of CO_2 loadings in liquid samples obtained with $BaCl_2$ titration method

4.3.1 Uncertainty of amine concentration

MEA concentration can be calculated using the equation (4-6) [45]:

$$C_{MEA} = \frac{V_{HCl} \cdot C_{HCl} \cdot M_{MEA}}{m_{sample}} \qquad (4\text{-}6)$$

Where:

V_{HCl} - consumed volume of 1M HCl, ml;

C_{HCl} - concentration of 1M HCl solution, mol/l;

M_{MEA} - molar mass of MEA, g/mol;

m_{sample} - mass of sample, g.

Four main sources of uncertainties for MEA concentration can be defined from equation (4-6): volume of 1M HCl, concentration of 1M HCl solution, molar mass of MEA and the mass of sample.

$$C_{MEA} = f(V_{HCl}, C_{HCl}, M_{MEA}, m_{sample})$$

Combined uncertainty for MEA concentration can be calculated with equation (4-7) [44]:

$$\frac{u_c(Y)}{Y} = \sqrt{\left(\frac{rep\,(Y)}{Y}\right)^2 + \sum_{i=1}^{n}\left(\frac{u(x_i)}{x_i}^2\right)} \qquad (4\text{-}7)$$

Where:

Y – analytical result;

rep(Y) - measurement repeatability;

x_i - uncertainty sources;

$u(x_i)$ - standard deviations of the uncertainty sources.

An extended version of equation (4-7) can be represented with equation (4-8) [45]:

$$\frac{u_c(C_{MEA})}{C_{MEA}} = \sqrt{\left(\frac{rep}{C_{MEA}}\right)^2 + \left(\frac{u(m_{sample})}{m_{sample}}\right)^2 + \left(\frac{u(V_{HCl})}{V_{HCl}}\right)^2 + \left(\frac{u(C_{HCl})}{C_{HCl}}\right)^2 + \left(\frac{u(M_{MEA})}{M_{MEA}}\right)^2} \qquad (4\text{-}8)$$

Where:

Rep – total repeatability for the whole analysis.

Repeatability, as discussed in reference [47], is defined as “a random error that manifests itself as differences in measured value from measurement to measurement during a measurement session”.

The values of MEA concentrations and loadings achieved with $BaCl_2$ titration are presented in the Appendix 5.

The average value of MEA concentration was calculated using titration results for 30% MEA sample №1 from Appendix 5:

$$\bar{C}_{MEA} = \frac{30.65 + 30.61}{2} = 30.63\,\frac{g(MEA)}{g(MEA + water)}$$

The standard deviation can be calculated with the equation (4-9) [44]:

$$s(x) = \sqrt{\frac{1}{N-1}\sum_{i=1}^{N}(x_i - \bar{x})^2} \qquad (4\text{-}9)$$

Where:

N- number of parallels;

x_i - concentration measurement;

$\bar{x}$ - mean value of concentration measurement.

As far as in this work 1 person performed the analysis for MEA samples 2 times, there is not enough data to determine the repeatability. Thus, the value of repeatability was taken equal to the value of repeatability for the worst case scenario from reference [45].

$$\frac{rep}{C_{MEA}} = 0.00043 = 0.043\%$$

Uncertainty of the mass sample was calculated in [28] with the assumption of rectangular distribution with the equation (4-10):

$$u(x) = a/\sqrt{3} \qquad (4\text{-}10)$$

Where:

$\mp a$ – the accuracy of the parameter.

The specified linearity of the Mettler Toledo XS403S analytical balance is 2 mg. The uncertainty was counted twice, for the empty beaker and the gross weight.

$$u(m_{sample}) = \sqrt{2 \cdot \left(\frac{2}{\sqrt{3}}\right)^2} = 1.633 \text{ mg} = 0.00163\text{g}$$

Uncertainty of the 1M HCl was calculated in [45] with the assumption of two sources:

- uncertainty due to the accuracy of the piston burette, which is ∓ 0.04 ml.

$$u(V_{HCl,cal}) = \frac{0.04}{\sqrt{6}} = 0.01633 \text{ ml}$$

- uncertainty of the difference between the laboratory temperature and calibration temperature($\mp 3^0 C$) with the coefficient of volume expansion for water $0.00021^0 C^{-1}$ and average consumed volume of 1M $V_{HCl} = 6.717$ ml.

$$V_{HCl} = \frac{6.694 + 6.74}{2} = 6.717 \text{ ml}$$

$$u(V_{HCl,temp}) = \frac{6.717 \text{ ml} \cdot 0.00021^0 C^{-1} \cdot 3^0 C}{\sqrt{3}} = 0.00345 \text{ ml}$$

Total uncertainty of the 1M HCl consumption was calculated with the equation (4-11) [43]:

$$u(V_{HCl}) = \sqrt{u(V_{HCl,cal})^2 + u(V_{HCl,temp})^2} \qquad (4\text{-}11)$$

$$u(V_{HCl}) = \sqrt{0.01633^2 + 0.00345^2} = 0.01669 \text{ ml}$$

Uncertainty of HCl concentration was calculated with the specified accuracy of Titrisol 1M HCl which is ∓ 0.002 M .

$$u(C_{HCl}) = \frac{0.002}{\sqrt{3}} = 0.00116 \text{ M}$$

Uncertainty of molar mass of MEA was calculated in [28]:

$$u(M_{MEA}) = 0.00101 \text{ g/mol}$$

Molar mass of MEA is equal $61.0828 \frac{g}{mol}$;

The average values of mass of the sample, consumed volume of 1M HCl and concentration of 1M HCl solution are calculated using data from Appendix 5:

$$m_{sample} = \frac{1.506 + 1.518}{2} = 1.512 \text{ g}$$

$$C_{HCl} = \frac{1+1}{2} = 1\ M$$

Standard uncertainty of the MEA concentration can be calculated with equation (4-8) using above calculated values of its constituents:

$$\frac{u_c(C_{MEA})}{C_{MEA}} = \sqrt{0.00043^2 + \left(\frac{0.00163}{1.512}\right)^2 + \left(\frac{0.01669}{6.717}\right)^2 + \left(\frac{0.00116}{1}\right)^2 + \left(\frac{0.00101}{61.0828}\right)^2} = 0.00166$$

Combined uncertainty for MEA concentration was calculated:

$$u_c(C_{MEA}) = C_{MEA} \cdot 0.00166 = 30.63 \cdot 0.00166 = 0.051 \frac{g(MEA)}{g(MEA + water)}$$

The expended uncertainty was calculated using the equation (4-2):

Thus,

$$U(C_{MEA}) = 0.00051 \cdot 2 = 0.1 \frac{g(MEA)}{g(MEA + water)}$$

Concentration of MEA is $30.6 \frac{g(MEA)}{g(MEA + water)} \mp 0.1 \frac{g(MEA)}{g(MEA + water)}$.

Based on the uncertainty calculations, the range of MEA concentration is from 30.5% to 30.7%.

4.3.2 Uncertainty of the loading analysis

The loading can be calculated with the equation (4-12) [45]:

$$\alpha_{CO_2} = \frac{((C_{HCl} \cdot V_{HCl} - C_{NaOH} \cdot V_{NaOH})_{sample} - (C_{HCl} \cdot V_{HCl} - C_{NaOH} \cdot V_{NaOH})_{blank}) \cdot M_{MEA}}{2 \cdot m_{sample} \cdot C_{MEA}} \qquad (4\text{-}12)$$

Where:

V_{HCl} - consumed volume of 0.1M HCl, ml;

C_{HCl} - concentration of 0.1M HCl solution, mol/l;

C_{NaOH} - concentration of 0.1M NaOH solution, mol/l;

V_{NaOH} - consumed volume of 0.1M NaOH, ml;

M_{MEA} - molar mass of MEA, g/mol;

m_{sample} - mass of sample, g.

The uncertainty of the loading analysis was calculated using equation (4-7). The extended form of the equation (4-7) was represented in [28] as is shown in equation (4-13):

$$\frac{u_c(\alpha_{CO\,2})}{\alpha_{CO\,2}} = \sqrt{\frac{rep}{\bar{\alpha}_{CO\,2}}^2 + \left(\frac{u(m_{sample})}{m_{sample}}\right)^2 + \left(\frac{u(C_{MEA})}{C_{MEA}}\right)^2 + 2\cdot\left(\frac{u(V_{HCl})}{V_{HCl}}\right)^2 + 2\cdot\left(\frac{u(C_{HCl})}{C_{HCl}}\right)^2 + 2\cdot\left(\frac{u(V_{NaOH})}{V_{NaOH}}\right)^2 + 2\cdot\left(\frac{u(C_{NaOH})}{C_{NaOH}}\right)^2 + \left(\frac{u(M_{MEA})}{M_{MEA}}\right)^2} \quad (4\text{-}13)$$

The uncertainty of volumes and concentrations are accounted twice, because of contribution to sample and to blank sample.

The average value of CO_2 loading was calculated using titration results for 30% MEA sample №1 from Appendix 5:

$$\bar{\alpha}_{CO\,2} = \frac{0.584+0.583}{2} = 0.583\,\frac{mol\ CO_2}{molMEA}$$

The value of repeatability was taken from [45] : $\frac{rep}{\bar{\alpha}_{CO\,2}} = 0.00696 = 0.0696\%$

The calculations of uncertainty for the 0.1M HCl and 0.1M NaOH volumes and concentrations, were performed with the same assumptions as for 1 M HCl in Section 4.3.1.

The uncertainty of the 0.1M HCl was calculated, considering the uncertainty of the accuracy of the piston burette and uncertainty of the difference between the laboratory temperature and calibration temperature:

$$u(V_{HCl,cal}) = \frac{0.04}{\sqrt{6}} = 0.01633\ ml$$

$$V_{HCl} = \frac{30.182 + 23.676}{2} = 26.929\ ml$$

$$u(V_{HCl,temp}) = \frac{26.929\ \text{ml} \cdot 0.00021^0C^{-1} \cdot 3^0\text{C}}{\sqrt{3}} = 0.01228\ \text{ml}$$

The total uncertainty of the 1M HCl consumption was calculated using equation (4-9):

$$u(V_{HCl}) = \sqrt{0.01633^2 + 0.01228^2} = 0.02043\ \text{ml}$$

The uncertainty of HCl concentration was calculated with the specified accuracy of Titrisol 1M HCl which is ∓ 0.002 M.

$$u(C_{HCl}) = \frac{0.0002}{\sqrt{3}} = 0.00012\ \text{M}$$

The uncertainty of the 0.1M NaOH was calculated, considering the uncertainty of the accuracy of the piston burette and uncertainty of the difference between the laboratory temperature and calibration temperature:

$$u(V_{NaOH,cal}) = \frac{0.02}{\sqrt{6}} = 0.00816\ \text{ml}$$

$$V_{NaOH} = \frac{12.847 + 6.742}{2} = 9.795\ \text{ml}$$

$$u(V_{NaOH,temp}) = \frac{9.795\ \text{ml} \cdot 0.00021^0C^{-1} \cdot 3^0C}{\sqrt{3}} = 0.00356\ \text{ml}$$

The total uncertainty of the 0.1M NaOH with equation (4-11):

$$u(V_{NaOH}) = \sqrt{0.00816^2 + 0.00356^2} = 0.00963\ \text{ml}$$

The uncertainty of NaOH concentration was calculated with the specified accuracy of Titrisol 0.1M NaOH which is ∓ 0.0001 M

$$u(C_{NaOH}) = \frac{0.0001}{\sqrt{3}} = 0.00006\ \text{M}$$

The average values of mass of the samples, consumed volumes of 0.1M HCl and 0.1M NaOH their concentrations are calculated using data from Appendix 5:

$$m_{sample} = \frac{0.316 + 0.309}{2} = 0.313 \text{ g}$$

$$C_{HCl} = C_{NaOH} = \frac{0.1 + 0.1}{2} = 0.1 \text{ M}$$

Found values are set in the equation (4-13):

$$\frac{u_c(\alpha_{CO_2})}{\alpha_{CO_2}} = \sqrt{0.00696^2 + \left(\frac{0.00163}{0.313}\right)^2 + 0.00785^2 + 2 \cdot \left(\frac{0.02043}{26.929}\right)^2 + 2 \cdot \left(\frac{0.00012}{0.1}\right)^2 + 2 \cdot \left(\frac{0.00963}{9.795}\right)^2 + 2 \cdot \left(\frac{0.00006}{0.1}\right)^2 + \left(\frac{0.00101}{61.0828}\right)^2}$$

$$\frac{u_c(\alpha_{CO_2})}{\alpha_{CO_2}} = 0.0092$$

The combined uncertainty for MEA concentration was calculated:

$$u_c(\alpha_{CO_2}) = \alpha_{CO_2} \cdot 0.006 = 0.583 \cdot 0.0092 = 0.0054 \frac{\text{mol } CO_2}{\text{mol MEA}}$$

The expanded uncertainty of CO_2 loading was calculated using the equation (4-2):

$$U(\alpha_{CO_2}) = 0.0054 \cdot 2 = 0.011 \frac{\text{mol } CO_2}{\text{mol MEA}}$$

The CO_2 loading in the liquid sample is $0.583 \frac{\text{mol } CO_2}{\text{mol MEA}} \mp 0.011 \frac{\text{mol } CO_2}{\text{mol MEA}}$.

Based on the uncertainty calculations, the range of α_{CO_2} is from 0.572 $\frac{\text{mol } CO_2}{\text{mol MEA}}$ to 0.594 $\frac{\text{mol } CO_2}{\text{mol MEA}}$.

Calculated values of CO_2 loading for each liquid sample are represented in Chapter 5.

5 Results and discussion

The solubility of CO_2 in aqueous MEA, MPA, 4A1B and 5A1P was measured in the laboratory using an equilibrium cell. Tables 5-1 – 5-4 show experimental data collected at 40 °C with calculated expanded uncertainties for CO_2 partial pressure (ΔP_{CO_2}) and CO_2 loading ($\Delta\alpha$). Vapor liquid equilibrium data from Jayarathna et al. [28] work for 30 % (wt) aqueous MEA at 40 °C is presented in the Table 5-5.

Table 5-1: Vapor liquid equilibrium data from this work for 30 % (wt) aqueous MEA at 40°C.

P_{CO_2}, kPa	ΔP_{CO_2}, kPa	α, mole CO_2 /mole MEA	$\Delta\alpha$, mole CO_2 /mole MEA	$P_{CO_2} - \Delta P_{CO_2}$, kPa	$P_{CO_2} + \Delta P_{CO_2}$, kPa	$\alpha - \Delta\alpha$	$\alpha + \Delta\alpha$
31.962	3.486	0.583	0.011	28.476	35.448	0.573	0.594
7.428	0.371	0.521	0.010	7.351	7.505	0.512	0.531
4.643	0.188	0.527	0.009	4.271	5.014	0.518	0.536
2.127	0.077	0.496	0.009	1.939	2.315	0.487	0.504
0.574	0.008	0.460	0.007	0.566	0.582	0.452	0.467
0.117	0.012	0.389	0.006	0.105	0.128	0.383	0.396

Table 5-2: Vapor liquid equilibrium data from this work for 30 % (wt) aqueous MPA at 40°C.

P_{CO_2}, kPa	ΔP_{CO_2}, kPa	α, mole CO_2 /mole MPA	$\Delta\alpha$, mole CO_2 /mole MPA	$P_{CO_2} - \Delta P_{CO_2}$, kPa	$P_{CO_2} + \Delta P_{CO_2}$, kPa	$\alpha - \Delta\alpha$	$\alpha + \Delta\alpha$
3.451	0.074	0.545	0.009	3.378	3.525	0.536	0.555
2.681	0.144	0.527	0.009	2.537	2.826	0.518	0.536
0.200	0.011	0.463	0.008	0.188	0.211	0.454	0.471
0.179	0.009	0.461	0.008	0.171	0.188	0.453	0.468
0.108	0.003	0.447	0.007	0.105	0.111	0.439	0.454
0.070	0.001	0.423	0.007	0.047	0.050	0.429	0.444
0.049	0.001	0.389	0.006	0.015	0.017	0.382	0.395
0.016	0.002	0.345	0.007	0.011	0.015	0.354	0.367
0.013	0.074	0.240	0.004	3.378	3.525	0.235	0.244

Table 5-3: Vapor liquid equilibrium data from this work for 30 % (wt) aqueous 4A1B at 40ºC.

P_{CO_2}, kPa	ΔP_{CO_2}, kPa	α, mole CO_2 /mole 4A1B	Δα, mole CO_2 /mole 4A1B	$P_{CO_2} - \Delta P_{CO_2}$, kPa	$P_{CO_2} + \Delta P_{CO_2}$, kPa	$\alpha - \Delta\alpha$	$\alpha + \Delta\alpha$
0.114	0.008	0.441	0.008	0.107	0.122	0.434	0.449
0.086	0.003	0.433	0.009	0.083	0.088	0.424	0.443
0.058	0.004	0.422	0.009	0.054	0.063	0.413	0.430
0.040	0.005	0.401	0.008	0.021	0.031	0.393	0.410
0.017	0.002	0.351	0.007	0.015	0.019	0.343	0.358
0.009	0.001	0.251	0.011	0.008	0.010	0.239	0.248
0.004	0.001	0.229	0.004	0.003	0.005	0.225	0.233

Table 5-4: Vapor liquid equilibrium data from this work for 30 % (wt) aqueous 5A1P at 40ºC.

P_{CO_2}, kPa	ΔP_{CO_2}, kPa	α, mole CO_2 /mole 5A1P	Δα, mole CO_2 /mole 5A1P	$P_{CO_2} - \Delta P_{CO_2}$, kPa	$P_{CO_2} + \Delta P_{CO_2}$, kPa	$\alpha - \Delta\alpha$	$\alpha + \Delta\alpha$
2.568	0.013	0.536	0.009	2.555	2.581	0.526	0.545
0.961	0.023	0.512	0.008	0.938	0.984	0.504	0.521
0.381	0.013	0.499	0.008	0.367	0.394	0.491	0.507
0.118	0.006	0.467	0.008	0.112	0.124	0.459	0.474
0.041	0.002	0.413	0.007	0.039	0.043	0.406	0.419
0.019	0.003	0.307	0.005	0.016	0.022	0.302	0.312
0.015	0.002	0.351	0.006	0.013	0.017	0.345	0.357
0.005	0.001	0.253	0.004	0.004	0.007	0.249	0.258

Table 5-5: Vapor liquid equilibrium data from Jayarathna et al. work for 30 % (wt) aqueous MEA at 40 ºC

P_{CO_2}, kPa	α, mole CO_2/mole MEA	$P_{CO_2} - \Delta P_{CO_2}$, kPa	$P_{CO_2} + \Delta P_{CO_2}$, kPa	$\alpha - \Delta\alpha$	$\alpha + \Delta\alpha$
0.0099	0.197	0.0083	0.0115	0.194	0.200
0.0146	0.213	0.0129	0.0162	0.210	0.216
0.0327	0.300	0.0307	0.0343	0.296	0.304
0.0515	0.332	0.0491	0.0531	0.328	0.336
0.2433	0.405	0.2346	0.2449	0.400	0.410
0.4351	0.437	0.4198	0.4367	0.431	0.443
2.9370	0.500	2.8342	2.9386	0.494	0.506
10.269	0.527	9.9096	10.271	0.520	0.534
15.593	0.540	15.047	15.595	0.533	0.547

The comparison of experimentally obtained VLE data for 30% MEA at 40 °C in this work and Jayarathna et al.[28] is presented in the Figure 5-1 and Figure 5-2. The gas phase analysis in both works was performed using the same GC equipment from Thermo-Scientific and liquid phase analysis with the same Mettler Toledo T50 titrator.

Figure 5-1 represents the logarithmic CO_2 partial pressure as a function of CO_2 loading in the range 0.2-0.6 mole CO_2/mole MEA.

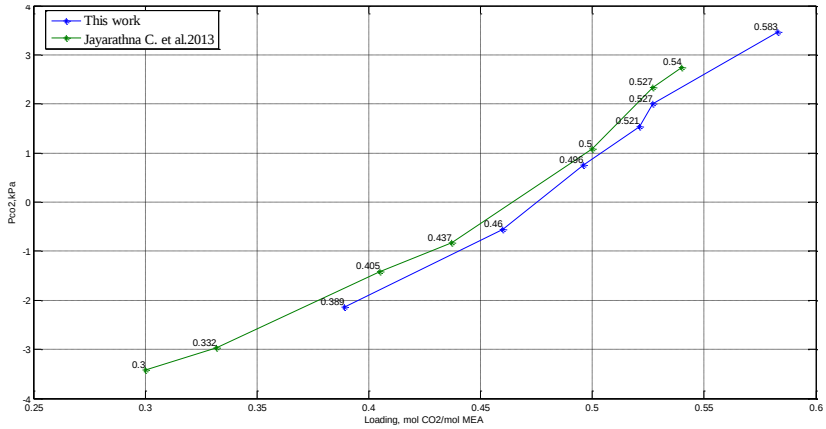

Figure 5-1: CO_2 partial pressures of 30% (wt) aqueous MEA at 40°C for the CO_2 loadings range 0.2-0.6 mole CO_2/mole MEA.

Figure 5-2 represents the CO_2 partial pressure as a function of CO_2 loading in the range 0.2-0.6 mole CO_2/mole MEA.

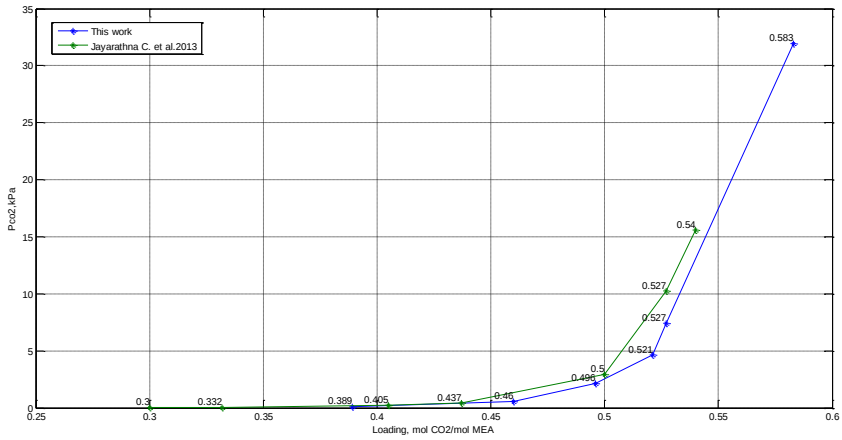

Figure 5-2: CO_2 partial pressures of 30% (wt) aqueous MEA at 40°C for the CO_2 loadings range 0.3-0.6 mole CO_2 /mole MEA.

As can be seen from the Figure 5-1 and Figure 5-2, measured values of CO_2 partial pressures in Jayarathna et al. [28] work are higher than the values of CO_2 partial pressures measured in this work for the same range of CO_2 loadings. The reason for the deviations in obtained results can be explained by systematic deviations over the time [44].

Figure 5-3 represents measured data of CO_2 partial pressures for 30% MEA at 40°C from different literature sources listed in Chapter 2, Table 2-1.

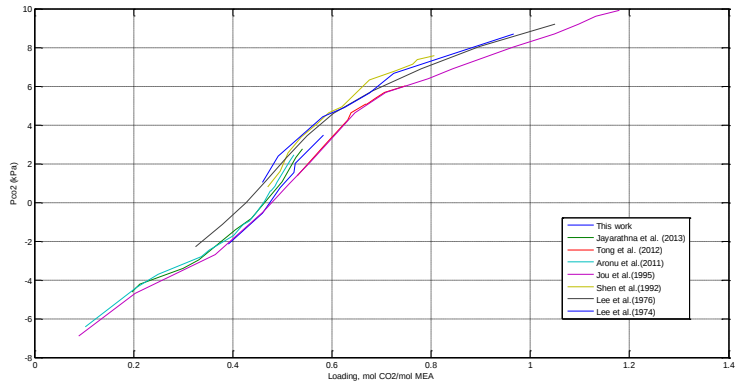

Figure 5-3: CO_2 partial pressures of 30% (wt) aqueous MEA at 40°C for the CO_2 loadings range 0.15-12 mole CO_2 /mole MEA.

The range of CO_2 loadings of CO_2 partial pressure curves represented in the Figure 5-2 is quite wide. Thus, for better analysis, Figure 5-4 represents CO_2 partial pressure curves in the CO_2 loading region 0.3-0.65 mole CO_2/mole MEA, more close to region, investigated in this work.

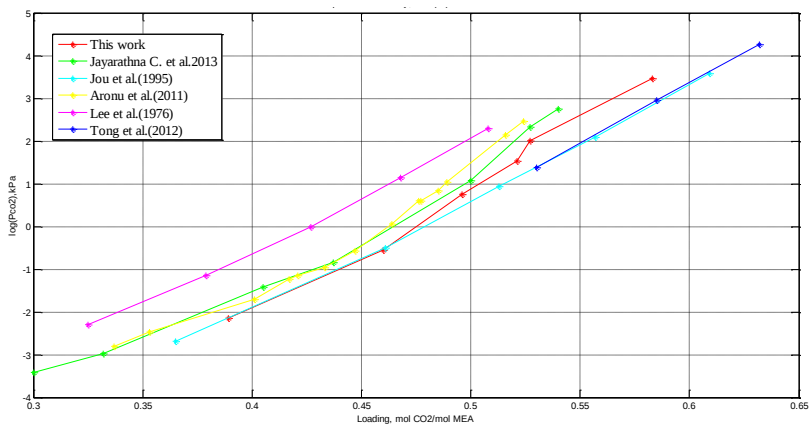

Figure 5-4: CO_2 partial pressures of 30% (wt) aqueous MEA at 40°C for the CO_2 loadings range 0.3-0.65 mole CO_2 /mole MEA.

Our results from this work are in best agreement with Jou et al.[21] for the CO_2 loading range 0.38-0.48 mole CO_2/mole MEA. For CO_2 loadings higher than 0.48, measured data in this

work is in the middle between the results of Jou et al. [21] and Jayarathna et al. [28] results. However, the measured data obtained by Jou et al.[21] for higher CO_2 agreed well with Tong et al [22].

The deviation of CO_2 partial pressures in the region of high CO_2 loadings can be explained with the fact, that the reactions of amine with CO_2 have different chemistry below and above 0.5 mole CO_2/mole MEA. The time constraint for reaching the VLE in carbamate region (CO_2 loading < 0.5 mole CO_2/ mole MEA) differs from the time constraint for reaching the VLE in bicarbonate region (CO_2 loading > 0.5 mole CO_2/ mole MEA). The reaction of bicarbonate formation, presented with the equation (1-3) is significantly slower than the reaction of carbamate formation, presented with the equation (1-4) [8, 48]. Thus, when the CO_2 loading is more than 0.5, higher time for reaching equilibrium is required.

Results, performed by Jayarathna et al. [28] are in good agreement with the results performed by Aronu et al [23].

The experimental results performed by Lee et al. [24] deviate considerably from the experimental results in this work and the rest results from other literature sources. The reason for such deviation was explained by Jou et al. [21] as the neglect of remaining CO_2 in the acidic solution during liquid phase analysis.

Figure 5-5 represents the equilibrium measurements of CO_2 partial pressures for 30% MPA at 40 °C temperatures. The results are compared with the only found literature data for 30 % and 15 % aqueous MPA at the same VLE conditions presented by Dong et al. [34].

Dong et al. used cell reactor for solubility measurements. Temperature control was performed with calibrated thermometer; pressure measurements – with calibrated pressure transducer respectively. It was assumed, that vapor-liquid equilibrium had been achivied after 10 hours of absorption.

Unfortunately, measurements taken by Dong et al. [34] are for CO_2 loadings in the region from 0.5 to 1 mol CO_2/mol MPA , while the CO_2 partial pressure measurements in this work are for CO_2 loading region from 0.27 to 0.55 mole CO_2/mole MPA.

30 % and 15% of aqueous MPA are equivalent to 4 $mol \cdot dm^3$ and 2 $mol \cdot dm^3$ of aqueous MPA respectively.

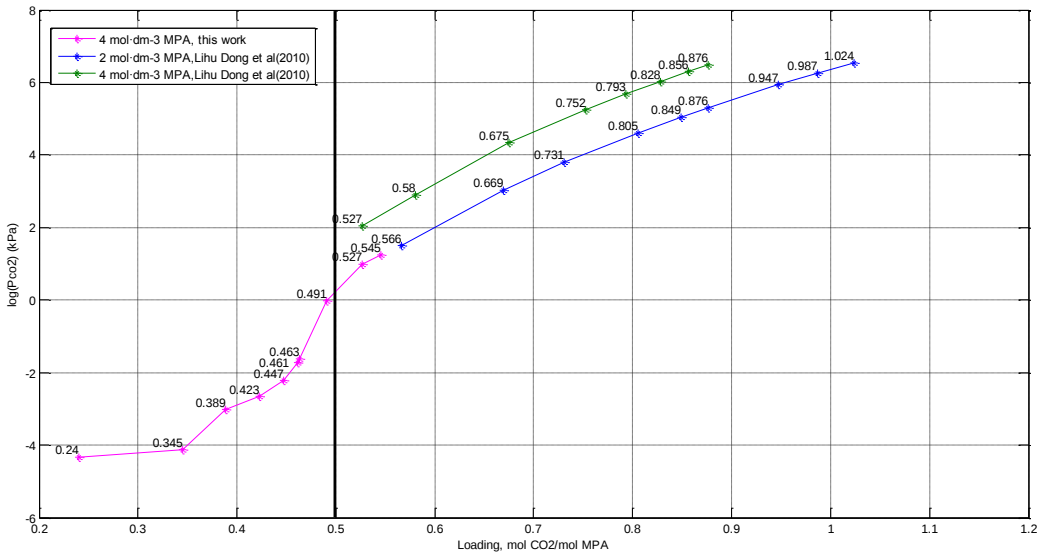

Figure 5-5: Equilibrium solubility, 30% (wt) aqueous MPA at 40°C.

Although there is a lack of data of CO_2 partial pressures for the CO_2 loading region investigated in this work, it can be seen from the Figure 5-5, that the CO_2 partial pressure values for 30% aqueous MPA in this work are more agreeable with CO_2 partial pressure values for 15% aqueous MPA than 30% aqueous MPA, published in [34].

Figure 5-6 represents partial pressure curves for 4 $mol \cdot dm^{-3}$ (30%) aqueous MPA obtained in this work, 2 $mol \cdot dm^{-3}$ and 4 $mol \cdot dm^{-3}$ (15% and 30% respectively) aqueous MPA from [22]. Zoomed in view for the 0.52-0.58 range of CO_2 loadings is represented on the Figure 5-6 as well.

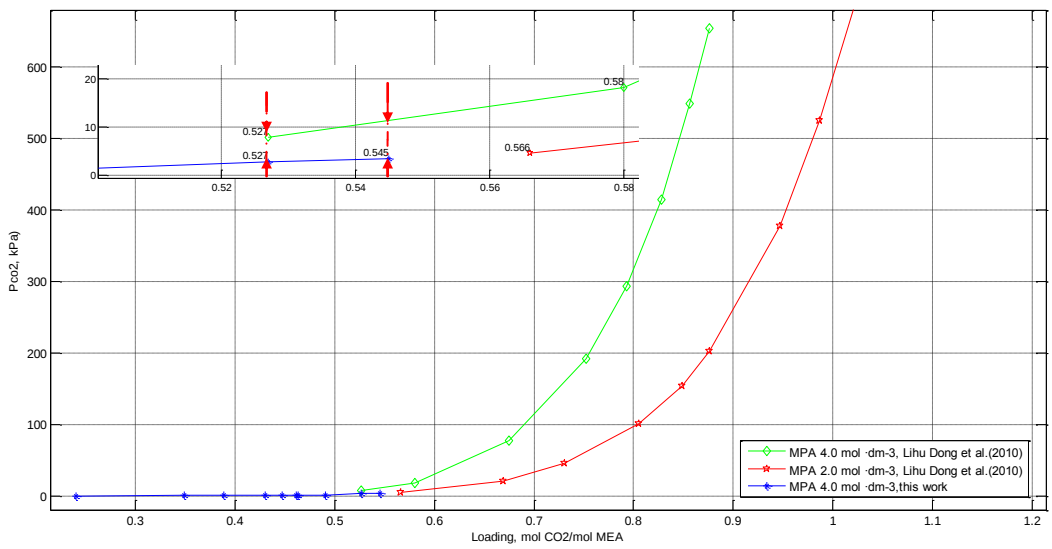

Figure 5-6: Equilibrium solubility, 30% (wt) aqueous MPA at 40°C.

It can be seen from the zoomed in view of curves in the Figure 5-6, that for the CO_2 loadings 0.527 and 0.545 the differences of partial pressure for 30% aqueous MPA in this work and in [22] equals to 7.7 kPa and 9.5 kPa respectively. The deviations of the results might be caused by differences in the used experimental techniques. It is also important to mention the anomalous sensitivity of CO_2 loading to partial pressure in the loading region higher 0.5 mole CO_2/mole amine.

The CO_2 loading range for 30% aqueous MEA investigated in this work is from 0.39 to 0.58, what is higher than the CO_2 loading range for the rest investigated amines. Thus, it was decided to compare VLE curves of 30% aqueous MPA, 4A1B and 5A1P, obtained in this work with 30% aqueous MEA VLE curve obtained by Jayarathna et al. [28].

Figure 5-7 represents the CO_2 partial pressure curves of 30 % aqueous MEA, MPA, 4A1B and 5A1P with CO_2 loading range 0.2-0.55 mole CO_2/mole amine.

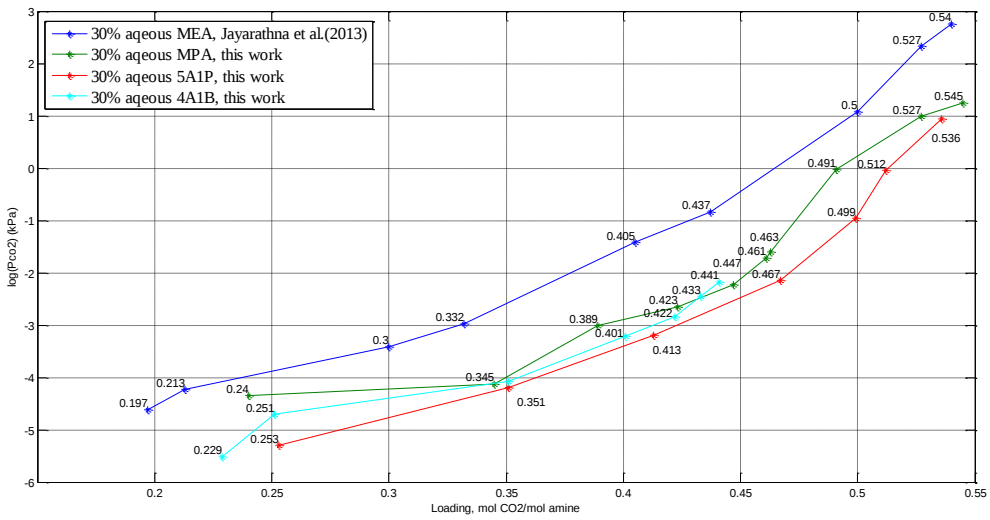

Figure 5-7: Equilibrium solubility, 30%(wt) aqueous MEA, MPA, 4A1B and 5A1P at 40 ℃.

Figure 5-7 shows that MEA possesses the highest CO_2 partial pressures in comparison to the rest investigated amines on the same loading region. It is also noticeable, that equilibrium curves of MPA and 4A1B are very close to each other. Even though isothermal MPA curve is higher than the 4A1B isothermal curve, in some points 4A1B curve crosses MPA curve. After 0.43 loading 4A1B curve performs tendency of higher CO_2 partial pressure values in comparison to MPA curve.

The influence of carbon chain length on amine absorption capacity is illustrated on the Figure 5-8 and Figure 5-9.

As can be seen from the Figure 5-8 and Figure 5-9, 5A1P has the highest CO_2 loadings in comparison to the rest 3 amines at the same partial pressures. For example, at absorption pressure 0.1 kPa, 5A1P has CO_2 loading 0.45 mole CO_2/mole amine. The CO_2 loadings of 4A1B and 3A1P are very close to 5A1P loading and equal to 0.43 and 0.44 respectively. MEA possess the lowest CO_2 loading of 0.35 mole CO_2/mole MEA at the same CO_2 partial pressure.

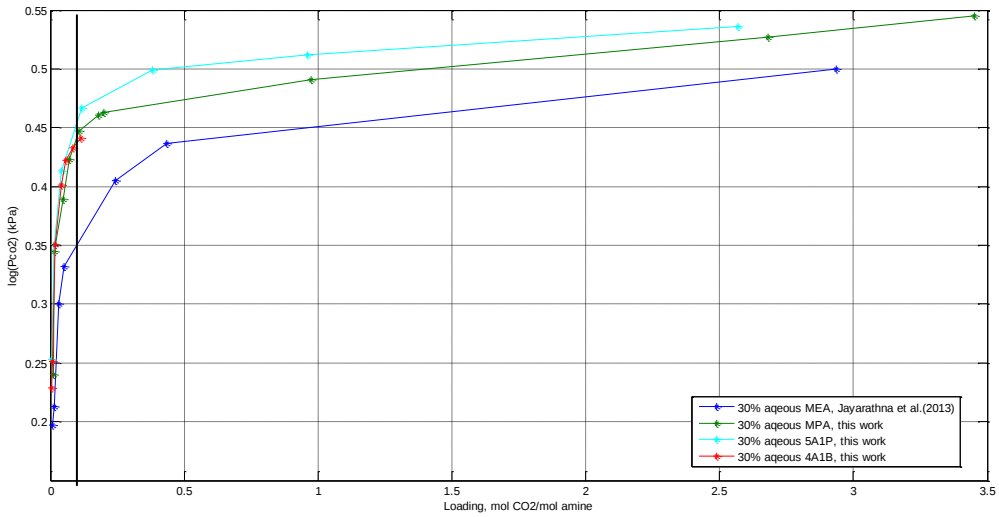

Figure 5-8: Equilibrium solubility, 30%(wt) aqueous MEA, MPA, 4A1B and 5A1P at 40 ^{0}C at CO_2 partial pressure range 0-3.5 kPa.

The comparison of investigated curves shows that there is a relation between CO_2 loading and the number of carbons in amine carbon chain. At constant partial pressure, the values CO_2 loading increase proportionally to the increase of the number of carbon atoms, from 2 carbon atoms in MEA chain to 5 carbon atoms in 5A1P. However, it is noticeable from the Figure 5-8, that isothermal curves of MPA, 4A1B and 5A1P lie very close to each other with quite similar values of CO_2 loadings.

Net capture capacities of investigated amines are shown on the Figure 5-9.

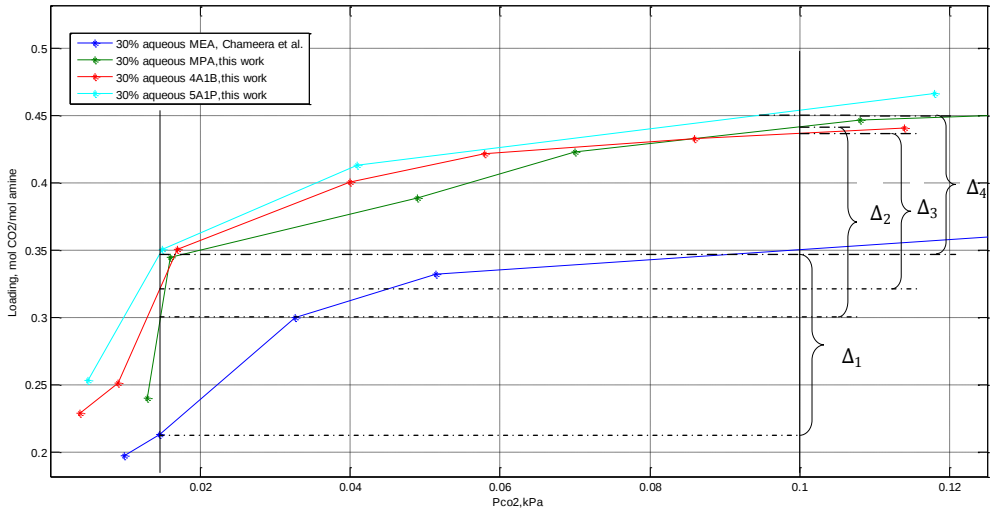

Figure 5-9: Equilibrium solubility, 30%(wt) aqueous MEA, MPA, 4A1B and 5A1P at 40 ^{o}C at CO_2 partial pressure range 0-0.12 kPa.

With the increase of partial pressure from 0.015 kPa to 0.1 kPa, the highest net capture capacity can be observed for MEA and MPA that are represented as Δ_1 and Δ_2 respectivaly in the Figure 5-9:

$$\Delta_1 = 0.35 - 0.21 = 0.14 \text{ mole } CO_2 / \text{ moleMEA}$$

$$\Delta_2 = 0.44 - 0.3 = 0.14 \text{ mole } CO_2 / \text{ mole MPA}$$

The net values of 4A1B and 5A1P net capture capacities, Δ_3 and Δ_4, equal to 0.12 and 0.10 mol CO_2 / mol amine respectively.

$$\Delta_3 = 0.44 - 0.32 = 0.12 \text{ mole } CO_2 / \text{ mole 4A1B}$$

$$\Delta_4 = 0.45 - 0.35 = 0.10 \text{ mole } CO_2 / \text{ mole 5A1P}$$

Analizing the values of CO_2 partial pressures uncertainties (ΔP_{CO_2}) and CO_2 loadings uncertainties ($\Delta\alpha$) reptesented in the Tables (5-1)- (5-5),and the CO_2 loading curves in the Figure 5-9, it can be seen, that the difference difference between the curves is higher than the difference between the uncertainties. Thus, it is reasonable to conclude that cyclic capacities of investigated amines have reverse relationship to the increase of amine carbon chain length, in spite of the fact that absolute loading capacity increases with the increase of the number of carbons in carbon chain.

6 Conclusion

CO_2 capture solvents, specifically primary amines with different carbon chain length have been studied in this Thesis. Amines MPA, 4A1B and 5A1P haven't been investigated enough and were chosen as solvents that may be useful for CO_2 capture technology. The Thesis includes literature review of available experimental data for investigated amines and literature research in the issue of structural change of amines on their CO_2 capture activities, VLE experiments, solvents characterization by means of absolute and cyclic loading capacity, uncertainty analysis of CO_2 partial pressures and loadings. All the experiments were performed for aqueous amine absorbents with 30% mass concentration at 40 ^{o}C.

Although a considerable amount of VLE literature data for MEA is available in literature resources, only one literature recourse with VLE data was found for MPA and none for 4A1B and 5A1P.

The MEA CO_2 partial pressure curve at equilibrium conditions in this work is in a good agreement with MEA curve in Jou et al.[21] for the CO_2 loading range 0.38-0.48 mole CO_2/mole MEA. However, for CO_2 loadings higher than 0.48, measured data in this work is in the middle between the results of Jou et al. [21] and Jayarathna et al. [28] results.

The obstacle to compare MPA VLE data in this work with already published data, is that the literature data for MPA are in the high region of CO_2 loadings what barely covers the region in this work. The comparison of MPA curves in the region 0.5-0.55 revealed significant deviations. Such deviations were explained with the differences in the used experimental techniques and sensitivity of CO_2 loading to partial pressure in the loading region higher 0.5 mole CO_2/mole amine.

The study of absolute and cyclic capacities of investigated amines in this work showed that absolute capacity have direct relationship to the increase of amine carbon chain length nevertheless cyclic capacity decreases with the increase of the number of carbons in carbon chain.

The results of this work can be further used for characterization, improvement and development of CO_2 absorbents.

7 Suggestion for further work

On the basis of the results in this work, the suggestions for further work are following :

- Obtained VLE data is not enough to make final judgment about investigated amines as alternatives to MEA and consequently, about the influence of structural change of amines on their CO_2 capture activities, thus:
    - VLE experiments on selected amines should be performed for higher range of CO_2 loadings;
    - This work performs the experiments for CO_2 solvents with constant mass concentration, the same solvents should be analyzed with constant molar concentration.
- More accurate measurements of CO_2 partial pressures with equilibrium cell could be performed by running the experiments from both absorption and desorption sides;
- The accuracy of the titration procedure should be increased with the performance of the sample titration a couple of times in specified period to avoid systematic deviations over the time;
- VLE data for middle and high pressures, valuable for industrial application, should be investigated in further works;
- The lack of VLE data can be compensated with the development of thermodynamic models.

References

1. Jos, G.J.O., J.-M. Greet, and A.H.W.P. Jeroen, *Trends in global CO_2 emissions*, P.N.E.A. Agency, Editor 2012.
2. Agency, I.E., *CO_2 emissions from fuel combustion* 2012.
3. IEA, *Evaluation of IEA ETP emission scenarios*, 2012.
4. Florin, N., *Review of Advanced Carbon Capture Technologies*, 2010, Imperial College.
5. Murrieta-Guevara, F., et al., *Solubility of CO_2 in aqueous mixtures of diethanolamine with methyldiethanolamine and 2-amino-2-methyl-1-propanol.* Fluid phase equilibria, 1998. **150**: p. 721-729.
6. Bellona. *Technology*. [cited 2013 11.02]; Available from: http://bellona.org/ccs/technology/capture/pre-combustion.html.
7. Rao, A.B. and E.S. Rubin, *A technical, economic, and environmental assessment of amine-based CO_2 capture technology for power plant greenhouse gas control.* Environmental Science & Technology, 2002. **36**(20): p. 4467-4475.
8. Kohl, A.L. and R.B. Nielsen, *Gas purification*. 1997: Gulf Professional Publishing.
9. Wang, M., et al., *Post-combustion CO_2 capture with chemical absorption: A state-of-the-art review.* Chemical Engineering Research and Design, 2011. **89**(9): p. 1609-1624.
10. D, V.P. and K.E. Y, *CO_2 - Alkanolamine Reaction Kinetics: A Review of Recent Studies.* Chemical Engineering & Technology, 2007. **30**(11): p. 1467-1474.
11. Sartori, G. and D.W. Savage, *Sterically hindered amines for carbon dioxide removal from gases.* Industrial & Engineering Chemistry Fundamentals, 1983. **22**(2): p. 239-249.
12. Ma'mun, S., et al., *Selection of new absorbents for carbon dioxide capture.* Energy conversion and management, 2007. **48**(1): p. 251-258.
13. Yang, Q., et al., *Influence of Amine Chemical Structures to Amine Capacities in CO_2 Capture*, in *Recent Advances in Post-Combustion CO_2 Capture Chemistry*. 2012, American Chemical Society. p. 29-42.
14. Singh, P., J.P. Niederer, and G.F. Versteeg, *Structure and activity relationships for amine based CO_2 absorbents—I.* International Journal of Greenhouse Gas Control, 2007. **1**(1): p. 5-10.
15. Singh, P., J.P. Niederer, and G.F. Versteeg, *Structure and activity relationships for amine-based CO_2 absorbents-II.* Chemical Engineering Research and Design, 2009. **87**(2): p. 135-144.
16. Singh, P. and G.F. Versteeg, *Structure and activity relationships for CO_2 regeneration from aqueous amine-based absorbents.* Process Safety and Environmental Protection, 2008. **86**(5): p. 347-359.
17. Chakraborty, A., G. Astarita, and K. Bischoff, *CO_2 absorption in aqueous solutions of hindered amines.* Chemical engineering science, 1986. **41**(4): p. 997-1003.
18. Hook, R.J., *An investigation of some sterically hindered amines as potential carbon dioxide scrubbing compounds.* Industrial & engineering chemistry research, 1997. **36**(5): p. 1779-1790.
19. Singh, P., D. Brilman, and M.J. Groeneveld, *Evaluation of CO_2 solubility in potential aqueous amine-based solvents at low CO_2 partial pressure.* International Journal of Greenhouse Gas Control, 2011. **5**(1): p. 61-68.

20. Øi, L.E., *Removal of CO_2 from exhaust gas*, in *Faculty of Technology*, Telemark University College: Porsgrunn.
21. Jou, F.Y., A.E. Mather, and F.D. Otto, *The solubility of CO2 in a 30 mass percent monoethanolamine solution.* The Canadian Journal of Chemical Engineering, 1995. **73**(1): p. 140-147.
22. Tong, D., et al., *Solubility of carbon dioxide in aqueous solution of monoethanolamine or 2-amino-2-methyl-1-propanol: Experimental measurements and modelling.* International Journal of Greenhouse Gas Control, 2012. **6**: p. 37-47.
23. Aronu, U.E., et al., *Solubility of CO_2 in 15, 30, 45 and 60 mass% MEA from 40 to 120° C and model representation using the extended UNIQUAC framework.* Chemical Engineering Science, 2011. **66**(24): p. 6393-6406.
24. Lee, J., F.D. Otto, and A.E. Mather, *The solubility of H2S and CO2 in aqueous monoethanolamine solutions.* The Canadian Journal of Chemical Engineering, 1974. **52**(6): p. 803-805.
25. Lee, J.I., F.D. Otto, and A.E. Mather, *Equilibrium between carbon dioxide and aqueous monoethanolamine solutions.* Journal of Applied Chemistry and Biotechnology, 1976. **26**(1): p. 541-549.
26. Shen, K.P. and M.H. Li, *Solubility of carbon dioxide in aqueous mixtures of monoethanolamine with methyldiethanolamine.* Journal of chemical and Engineering Data, 1992. **37**(1): p. 96-100.
27. Jayarathna, C. and L. Andersen, *GAI 15 Equilibrium Cell instructions*, Tel-Tek, Editor 2012: Porsgrunn.
28. Jayarathna, C., et al., *Experimentally based evaluation of accuracy of absorption equilibrium measurements*, in *International conference on greenhouse gas technologies (GHGT)* 2013: Kyoto.
29. Elverhøy, A.B., *Procedure - operating titrator T50 for loading and MEA concentration analysis*, Tel-Tek, Editor: Porsgrunn.
30. Elverhøy, A.B., *Liquid phase CO_2 loading analysis by using the $BaCl_2$ method for total alkalinity*, Tel-Tek, Editor.
31. Elverhøy, A.B., *Procedure - operating titrator*, Tel-Tek: Porsgrunn.
32. Ma'mun, S., et al., *Experimental and modeling study of the solubility of carbon dioxide in aqueous 30 mass% 2-((2-aminoethyl) amino) ethanol solution.* Industrial & engineering chemistry research, 2006. **45**(8): p. 2505-2512.
33. Camacho, F., S. Sanchez, and R. Pacheco, *Thermal effects during the absorption of CO_2 in aqueous solutions of 3-amino-1-propanol.* Chemical engineering & technology, 2000. **23**(12): p. 1073-1080.
34. Dong, L., J. Chen, and G. Gao, *Solubility of carbon dioxide in aqueous solutions of 3-amino-1-propanol.* Journal of Chemical & Engineering Data, 2009. **55**(2): p. 1030-1034.
35. Kadiwala, S., A.V. Rayer, and A. Henni, *Kinetics of carbon dioxide (CO_2) with ethylenediamine, 3-amino-1-propanol in methanol and ethanol, and with 1-dimethylamino-2-propanol and 3-dimethylamino-1-propanol in water using stopped-flow technique.* Chemical Engineering Journal, 2012. **179**: p. 262-271.
36. Ma'mun, S., *Selection and characterization of new absorbents for carbon dioxide capture*, 2005, Norwegian University of Science and Technology.
37. TutorVista.com. *Gas chromotography*. 2013 [cited 2013 26 May]; Available from: http://chemistry.tutorvista.com/analytical-chemistry/chromotography.html.

38. About.com, C. *Acids and Bases - Titration Curves*. [cited 2013 26 May]; Available from: http://chemistry.about.com/od/acidsbase1/ss/titrationcurves.htm.

39. Ma'mun, S., et al., *Solubility of carbon dioxide in 30 mass% monoethanolamine and 50 mass% methyldiethanolamine solutions.* Journal of Chemical & Engineering Data, 2005. **50**(2): p. 630-634.

40. Bipm, I., et al., *Guide to the expression of uncertainty in measurement.* ISO, Geneva, 1993.

41. Gum, I., *Guide to the expression of uncertainty in measurement.* BIPM, IEC, IFCC, ISO, IUPAP, IUPAC, OIML, 1995.

42. BIPM, I., I. IFCC, and I. ISO, *IUPAP and OIML, Evaluation of measurement data-Guide to the expression of uncertainty in measurement.* International Organization for Standardization (ISO), Online: http://www.bipm.org/en/publications/guides/gum.html, 2008.

43. Ellison, S.L., M. Rosslein, and A. Williams, *Quantifying uncertainty in analytical measurement.* 2000.

44. Meyer, V.R., *Measurement uncertainty.* Journal of Chromatography A, 2007. **1158**(1): p. 15-24.

45. Elverhøy, A.B., *Introducrion to Uncertainty Analysis, QUAM method*, Unpublished, Editor 2011, Tel-Tek: Porsgrunn, Norway,.

46. Taylor, B.N., *Guidelines for Evaluating and Expressing the Uncertainty of NIST Measurement Results (rev*. 2009: DIANE Publishing.

47. NASA, *Measurement Uncertainty Analysis Principles and Methods, NASA Measurement Quality Assurance Handbook – ANNEX 3*, 2010, National aeronautics and space administration: Washington DC 20546. p. 248.

48. McCann, N., et al., *Kinetics and mechanism of carbamate formation from CO2 (aq), carbonate species, and monoethanolamine in aqueous solution.* The Journal of Physical Chemistry A, 2009. **113**(17): p. 5022-5029.

Appendices

Appendix 1: Task paper

Appendix 2: Equilibrium measurements of CO_2 partial pressure for 30% Monoethanolamine at 40 °C with calculated expanded uncertainty

Appendix 3: Equilibrium measurements of CO_2 partial pressure for 30% 3-Amino-1-propanol at 40 °C with calculated expanded uncertainty

Appendix 4: Equilibrium measurements of CO_2 partial pressure for 30% 4-Amino-1-butanol at 40 °C with calculated expanded uncertainty

Appendix 5: Equilibrium measurements of CO_2 partial pressure for 30% 5-Amino-1-pentanol at 40 °C with calculated expanded uncertainty

Appendix 6: $BaCl_2$ titration results of CO_2 loadings and concentrations for Monoethanolamine liquid samples

Appendix 7: $BaCl_2$ titration results of CO_2 loadings and concentrations for 3-Amino-1-propanol liquid samples

Appendix 8: $BaCl_2$ titration results of CO_2 loadings and concentrations for 4-Amino-1-butanol liquid samples

Appendix 9: $BaCl_2$ titration results of CO_2 loadings and concentrations for 5-Amino-1-pentanol liquid samples

Appendix 1: Task paper

Telemark University College

Faculty of Technology

FMH606 Master's Thesis

Title: CO_2 capture solvent performance characterization

TUC supervisor: Klaus-J. Jens; Zul Idris

External partner: Tel-Tek

Task description:

New solvent formulations will be identified in co-operation with the supervisors. The solvent(s) shall be characterized by measurement of CO_2-solvent vapour-liquid-equilibria (VLE) curves. If time allows, VLE curves shall be supplemented with selected other solvent characterization techniques (i.e. CO_2 desorption energy).

Task background:

Identification of low cost and energy efficient CO_2 capture mechanisms and/or adsorbants is one of today's important research topics. A current commercial process for CO_2 capture utilizes absorption of CO_2 in MEA (mono-ethanolamine) solution. MEA solutions slowly decompose during service and significant energy is required for the CO_2 desorption step. Thus there is a need to identify improved CO_2 capture systems.

Student category:

PT or EET students

Practical arrangements:

Solvent characterization equipment is available in the CO_2 laboratory.

Signatures:

Student (date and signature): 28-01.2012 N. Tong

Supervisor (date and signature): 28.01.2012

29.01.2013

Address: Kjølnes ring 56, NO-3918 Porsgrunn, Norway. **Phone:** 35 57 50 00. **Fax:** 35 55 75 47.

Appendix 2: Equilibrium measurements of CO_2 partial pressure for 30% Monoethanolamine at 40 °C with calculated expanded uncertainty[1].

sample	P_{CO2}, kPa	Average P_{CO2}, kPa	Rel. Std. Dev, %	$\frac{Uc}{p_{CO2}}$	uc, kPa	U, kPa
s1	30.9166	31.962	5.448	0.055	1.743	3.486
	33.9721					
	30.9968					
s2	4.8005	4.643	3.993	0.040	0.186	0.040
	4.6886					
	4.4384					
s3	2.2351	2.127	4.411	0.044	0.094	0.188
	2.0791					
	2.0668					
s4	7.4493	7.428	0.454	0.005	0.038	0.077
	7.3851					
	7.4493					
s5	0.5722	0.574	0.671	0.007	0.004	0.008
	0.5787					
	0.5719					
s6	0.1116	0.117	5.021	0.050	0.006	0.012
	0.1235					
	0.1195					
	0.1119					

[1] The definition of symbols in the table is presented in the nomenclature

Appendix 3: Equilibrium measurements of CO_2 partial pressure for 30% 3-amino-1-propanol at 40 °C with calculated expanded uncertainty.

sample	P_{CO2}, kPa	Average P_{CO2}, kPa	Rel. Std. Dev, %	$\frac{Uc}{p_{CO2}}$	uc, kPa	U, kPa
s1	3.4356	3.451	1.040	0.003	0.0086	0.0173
	3.4675					
	3.4924					
	3.4104					
s2	0.2056	0.200	2.827	0.028	0.0057	0.0113
	0.1984					
	0.1945					
s3	0.0494	0.049	1.392	0.014	0.0007	0.0014
	0.0483					
	0.049					
	0.0479					
	0.0479					
s4	0.0166	0.016	3.329	0.033	0.0005	0.0011
	0.0161					
	0.0154					
	0.0164					
s5	0.0138	0.013	8.010	0.080	0.0010	0.0021
	0.0118					
	0.0128					
s6	2.6191	2.681	2.681	0.027	0.0722	0.1444
	2.6545					
	2.6673					
	2.7849					
s9	0.1835	0.179	2.363	0.024	0.0043	0.0085
	0.1751					
	0.1788					
s10	0.1078	0.108	1.275	0.013	0.0014	0.0028
	0.1095					
	0.1062					
	0.1074					
s11	0.0669	0.070	3.428	0.034	0.0024	0.0048
	0.0687					
	0.0732					
	0.0720					
	0.0682					
	0.0696					

Appendix 4: Equilibrium measurements of CO_2 partial pressure for 30% 4-amino-1-butanol at 40 °C with calculated expanded uncertainty.

sample	P_{CO2}, kPa	Average P_{CO2}, kPa	Rel. Std. Dev, %	$\frac{Uc}{p_{CO2}}$	uc, kPa	U, kPa
1	0.120 0.111 0.116 0.111 0.114	0.114	3.373	0.034	0.00386	0.008
2	0.086 0.086 0.086 0.084 0.088 0.085	0.086	1.501	0.015	0.00131	0.003
3	0.060 0.061 0.057 0.056	0.058	3.752	0.038	0.00219	0.004
4	0.039 0.039 0.039 0.041	0.040	2.830	0.028	0.00113	0.002
5	0.016 0.018 0.017 0.018	0.017	6.130	0.061	0.00106	0.002
6	0.009 0.009 0.009 0.009	0.009	3.138	0.031	0.00028	0.001
7	0.005 0.004 0.004 0.004	0.004	10.721	0.107	0.00043	0.001
8	0.028 0.024	0.026	9.579	0.096	0.00252	0.005

Appendix 5: Equilibrium measurements of CO_2 partial pressure for 30% 5-Amino-1-pentanol at 40 ℃ with calculated expanded uncertainty.

sample	P_{CO2}, kPa	Average P_{CO2}, kPa	Rel. Std. Dev, %	$\frac{Uc}{p_{CO2}}$	uc, kPa	U, kPa
s1	2.6182	2.568	2.014	0.003	0.006	0.013
	2.5964					
	2.5006					
	2.5555					
s2	0.9715	0.961	1.173	0.012	0.012	0.023
	0.974					
	0.948					
	0.9601					
	0.9534					
s3	0.3714	0.381	1.715	0.017	0.007	0.013
	0.3854					
	0.3807					
	0.3851					
s4	0.1184	0.118	2.555	0.026	0.003	0.006
	0.1176					
	0.1135					
	0.1207					
s5	0.0407	0.041	2.396	0.024	0.001	0.002
	0.0423					
	0.0405					
	0.0423					
	0.0404					
s6	0.0156	0.015	6.238	0.062	0.001	0.002
	0.0162					
	0.0147					
	0.0138					
	0.0146					
s7	0.0056	0.005	13.158	0.132	0.001	0.001
	0.0045					
	0.0058					
s8	0.0204	0.019	7.720	0.077	0.001	0.003
	0.018					
	0.0178					

Appendix 6: $BaCl_2$ titration results of CO_2 loadings and concentrations for 30 (wt) % Monoethanolamine liquid samples.

Sample	s1		s2		s3		s4		s5		s6	
C_{HCl}, mol	0.1	0.1	0.1	0.1	0.1	0.1	0.1	0.1	0.1	0.1	0.1	0.1
V_{HCl}, ml	30.182	23.676	24.59	28.433	28.867	26.003	44.295	44.422	39.877	38.885	25.584	36.585
V_{HCl} blank sample, ml	11.809	11.809	11.809	11.809	11.809	11.809	16.766	16.766	16.766	16.766	13.293	13.293
C_{NaOH}, mol	0.1	0.1	0.1	0.1	0.1	0.1	0.1	0.1	0.1	0.1	0.1	0.1
V_{NaOH}, ml	12.847	6.742	9.284	13.41	13.793	11.484	19.386	19.815	17.622	16.748	7.128	17.418
V_{NaOH}, blank sample, ml	10.875	10.875	10.875	10.875	10.875	10.875	15.806	15.806	15.806	15.806	12.631	12.631
M_{CO2}, g/mol	44.01	44.01	44.01	44.01	44.01	44.01	44.01	44.01	44.01	44.01	44.01	44.01
$m_{sample\ loading}$, g	0.316	0.309	0.308	0.3	0.316	0.303	0.506	0.502	0.509	0.506	0.499	0.51
n(CO_2 in sample), mol	0.00087	0.00085	0.00077	0.00075	0.00075	0.00073	0.00125	0.00123	0.00111	0.00111	0.00092	0.00096
n(CO_2 in blank sample), mol	0.00005	0.00005	0.00005	0.00005	0.00005	0.00005	0.00005	0.00005	0.00005	0.00005	0.00003	0.00003
m(CO_2 in blank sample), g	0.00206	0.00206	0.00206	0.00206	0.00206	0.00206	0.00211	0.00211	0.00211	0.00211	0.00146	0.00146
m(CO_2 in sample), g	0.03609	0.03521	0.03163	0.03100	0.03112	0.02989	0.05270	0.05204	0.04686	0.04660	0.03916	0.04072
$M_{MEA+water}$, g/mol	0.27991	0.27379	0.27637	0.26900	0.28488	0.27311	0.45330	0.44996	0.46214	0.45940	0.45984	0.46928
$n_{CO2}/m_{MEA+water}$	2.92970	2.92193	2.60010	2.61880	2.48170	2.48713	2.64163	2.62765	2.30395	2.30485	1.93479	1.97164
f	0.11421	0.11394	0.10268	0.10334	0.09847	0.09866	0.10415	0.10366	0.09206	0.09209	0.07847	0.07984
C_{HCl}, mol	1	1	1	1	1	1	1	1	1	1	1	1
V_{HCl}, ml	6.694	6.74	6.786	6.799	6.778	6.789	9.042	9.045	9.149	9.199	9.217	9.28
M_{MEA}, g/mol	61.08	61.08	61.08	61.08	61.08	61.08	61.08	61.08	61.08	61.08	61.08	61.08
$m_{MEA.cons}$, g	0.40887	0.41168	0.41449	0.41528	0.41400	0.41467	0.55229	0.55247	0.55882	0.56187	0.56297	0.56682
$m_{sample.cons}$, g	1.506	1.518	1.513	1.513	1.503	1.501	2.0186	2.0201	2.011	2.021	2.002	2.0005
$m_{MEA+water.cons}$, g	1.33400	1.34504	1.35764	1.35664	1.35501	1.35291	1.80836	1.81070	1.82586	1.83488	1.84491	1.84077
wt%MEA	30.650	30.607	30.530	30.611	30.553	30.650	30.541	30.511	30.606	30.622	30.515	30.793
$n_{MEA}/m_{MEA+water}$	5.01799	5.01102	4.99836	5.01164	5.00219	5.01806	5.00010	4.99529	5.01078	5.01342	4.99592	5.04136
$\alpha, \frac{mol\ CO_2}{mol\ MEA}$	0.584	0.583	0.520	0.523	0.496	0.496	0.528	0.526	0.460	0.460	0.387	0.391

Appendix 7: $BaCl_2$ titration results of CO_2 loadings and concentrations for 30 wt % 3-amino-1-propanol liquid samples.

Sample	s1	s1	s1	s2	s2	s2	s3	s3	s3
C_{HCl}, mol	0.1	0.1	0.1	0.1	0.1	0.1	0.1	0.1	0.1
V_{HCl}, ml	44.604	30.263	24.998	27.942	28.965	25.311	32.085	32.818	34.277
V_{HCl} blank sample, ml	15.060	15.060	15.060	13.595	13.595	13.595	14.347	14.347	14.347
C_{NaOH}, mol	0.1	0.1	0.1	0.1	0.1	0.1	0.1	0.1	0.1
V_{NaOH}, ml	19.136	16.757	15.976	16.333	17.043	13.645	16.613	17.141	18.163
V_{NaOH}, blank sample, ml	14.612	14.612	14.612	12.885	12.885	12.885	13.562	13.562	13.562
M_{CO2}, g/mol	44.01	44.01	44.01	44.01	44.01	44.01	44.01	44.01	44.01
$m_{sample\ loading}$, g	0.614	0.313	0.207	0.310	0.318	0.309	0.500	0.501	0.519
n(CO_2 in sample), mol	0.00127	0.00068	0.00045	0.00058	0.00060	0.00058	0.00077	0.00078	0.00081
n(CO_2 in blank sample), mol	0.00002	0.00002	0.00002	0.00004	0.00004	0.00004	0.00004	0.00004	0.00004
m(CO_2 in blank sample), g	0.00099	0.00099	0.00099	0.00156	0.00156	0.00156	0.00173	0.00173	0.00173
m(CO_2 in sample), g	0.05506	0.02873	0.01887	0.02398	0.02467	0.02411	0.03232	0.03277	0.03373
$M_{amine+water}$, g/mol	0.55894	0.28427	0.18813	0.28602	0.29333	0.28489	0.46768	0.46823	0.48527
$n_{CO2}/m_{amine+water}$	2.23815	2.29679	2.27871	1.90531	1.91117	1.92284	1.57019	1.59024	1.57943
f	0.08967	0.09180	0.09115	0.07737	0.07758	0.07802	0.06464	0.06541	0.06499
C_{amine}, mol	1	1	1	1	1	1	1	1	1
V_{amine}, ml	5.668	5.673	5.673	5.72	5.75	5.882	5.744	5.701	5.721
M_{amine}, g/mol	75.11	75.11	75.11	75.11	75.11	75.11	75.11	75.11	75.11
$m_{amine.cons}$, g	0.426	0.426	0.426	0.430	0.432	0.442	0.431	0.428	0.430
$m_{sample.cons}$, g	1.505	1.495	1.495	1.506	1.513	1.529	1.508	1.501	1.507
$m_{amine+water.cons}$, g	1.370	1.358	1.359	1.389	1.396	1.410	1.411	1.403	1.409
wt% amine	31.074	31.383	31.360	30.920	30.946	31.340	30.587	30.524	30.496
$n_{amine}/m_{amine+water}$	4.137	4.178	4.175	4.117	4.120	4.173	4.072	4.064	4.060
$\alpha, \frac{\text{mol } CO_2}{\text{mol amine}}$	0.541	0.550	0.546	0.463	0.464	0.461	0.386	0.391	0.389

Appendix 7 (continied).

Sample	s4	s4	s4	s5	s5	s5	s6	s6	s6
C_{HCl}, mol	0.1	0.1	0.1	0.1	0.1	0.1	0.1	0.1	0.1
V_{HCl}, ml	30.795	29.84	29.147	26.527	21.947	26.767	33.309	33.328	34.008
V_{HCl} blank sample, ml	12.56	12.56	12.56	14.668	14.668	14.668	13.055	13.055	13.055
C_{NaOH}, mol	0.1	0.1	0.1	0.1	0.1	0.1	0.1	0.1	0.1
V_{NaOH}, ml	16.594	15.374	14.623	16.396	12.396	17.628	16.771	16.613	17.666
V_{NaOH}, blank sample, ml	11.652	11.652	11.652	14.08	14.08	14.08	12.489	12.489	12.489
M_{CO2}, g/mol	44.01	44.01	44.01	44.01	44.01	44.01	44.01	44.01	44.01
$m_{sample\ loading}$, g	0.509	0.512	0.516	0.433	0.422	0.403	0.407	0.403	0.4
n(CO_2 in sample), mol	0.00071	0.00072	0.00073	0.00051	0.00048	0.00046	0.00083	0.00084	0.00082
n(CO_2 in blank sample), mol	0.00005	0.00005	0.00005	0.00003	0.00003	0.00003	0.00003	0.00003	0.00003
m(CO_2 in blank sample), g	0.00200	0.00200	0.00200	0.00129	0.00129	0.00129	0.00125	0.00125	0.00125
m(CO_2 in sample), g	0.02925	0.02983	0.02996	0.02100	0.01972	0.01882	0.03515	0.03554	0.03472
$M_{amine+water}$, g/mol	0.47975	0.48217	0.48604	0.41200	0.40228	0.38418	0.37185	0.36746	0.36528
$n_{CO2}/m_{amine+water}$	1.38541	1.40595	1.40071	1.15813	1.11403	1.11288	2.14762	2.19736	2.15941
f	0.05747	0.05827	0.05807	0.04850	0.04674	0.04669	0.08635	0.08818	0.08679
C_{amine}, mol	1	1	1	1	1	1	1	1	1
V_{amine}, ml	6.057	5.755	5.762	7.117	7.117	7.117	5.603	5.644	5.674
M_{amine}, g/mol	75.11	75.11	75.11	75.11	75.11	75.11	75.11	75.11	75.11
$m_{amine.cons}$, g	0.455	0.432	0.433	0.535	0.535	0.535	0.421	0.424	0.426
$m_{sample.cons}$, g	1.586	1.507	1.507	1.586	1.586	1.586	1.506	1.497	1.506
$m_{amine+water.cons}$, g	1.495	1.419	1.419	1.509	1.512	1.512	1.376	1.365	1.375
wt% amine	30.434	30.458	30.489	35.423	35.357	35.356	30.586	31.057	30.988
$n_{amine}/m_{amine+water}$	4.052	4.055	4.059	4.716	4.707	4.707	4.072	4.135	4.126
$\alpha, \frac{mol\ CO_2}{mol\ amine}$	0.342	0.347	0.345	0.246	0.237	0.236	0.527	0.531	0.523

Appendix 7 (contined).

Sample	S7	S7	S7	S8	S8	S8	s9	S9	S9	S9	S9	S9
C_{HCl}, mol	0.1	0.1	0.1	0.1	0.1	0.1	0.1	0.1	0.1	0.1	0.1	0.1
V_{HCl}, ml	37.946	36.643	35.68	37.928	35.219	36.666	32.117	32.548	31.413	29.772	32.25	32.976
V_{HCl} blank sample, ml	16.764	16.764	16.764	16.764	16.764	16.764	12.56	12.56	9.664	14.347	14.347	14.347
C_{NaOH}, mol	0.1	0.1	0.1	0.1	0.1	0.1	0.1	0.1	0.1	0.1	0.1	0.1
V_{NaOH}, ml	20.139	18.505	17.564	20.612	17.73	19.34	14.851	15.434	14.198	13.976	16.244	17.1
V_{NaOH}, blank sample, ml	16.339	16.339	16.339	16.339	16.339	16.339	11.562	11.562	8.941	13.562	13.562	13.562
M_{CO2}, g/mol	44.01	44.01	44.01	44.01	44.01	44.01	44.01	44.01	44.01	44.01	44.01	44.01
$m_{sample\ loading}$, g	0.501	0.511	0.509	0.501	0.505	0.5	0.508	0.503	0.506	0.405	0.41	0.409
n(CO_2 in sample), mol	0.00089	0.00091	0.00091	0.00087	0.00087	0.00087	0.00086	0.00086	0.00086	0.00079	0.00080	0.00079
n(CO_2 in blank sample), mol	0.00002	0.00002	0.00002	0.00002	0.00002	0.00002	0.00005	0.00005	0.00005	0.00004	0.00004	0.00004
m(CO_2 in blank sample), g	0.00094	0.00094	0.00094	0.00094	0.00094	0.00094	0.00220	0.00220	0.00220	0.00173	0.00173	0.00173
m(CO_2 in sample), g	0.03825	0.03898	0.03893	0.03717	0.03755	0.03719	0.03580	0.03546	0.03569	0.03303	0.03349	0.03321
$M_{amine+water}$, g/mol	0.46275	0.47202	0.47007	0.46383	0.46745	0.46281	0.47220	0.46754	0.47031	0.37197	0.37651	0.37579
$n_{CO2}/m_{amine+water}$	1.87812	1.87629	1.88174	1.82081	1.82522	1.82591	1.72257	1.72350	1.72406	2.01778	2.02135	2.00789
f	0.07635	0.07628	0.07648	0.07419	0.07436	0.07438	0.07047	0.07050	0.07052	0.08156	0.08169	0.08119
C_{amine}, mol	1	1	1	1	1	1	1	1	1	1	1	1
V_{amine}, ml	5.661	5.649	5.701	5.705	5.726	5.724	5.756	5.721	5.753	6.064	6.098	6.162
M_{amine}, g/mol	75.11	75.11	75.11	75.11	75.11	75.11	75.11	75.11	75.11	75.11	75.11	75.11
$m_{amine.cons}$, g	0.425	0.424	0.428	0.429	0.430	0.430	0.432	0.430	0.432	0.455	0.458	0.463
$m_{sample.cons}$, g	1.503	1.502	1.510	1.518	1.507	1.514	1.522	1.511	1.520	1.613	1.618	1.628
$m_{amine+water.cons}$, g	1.388	1.387	1.395	1.405	1.395	1.401	1.415	1.404	1.413	1.481	1.486	1.496
wt% amine	30.628	30.581	30.706	30.490	30.831	30.679	30.559	30.595	30.585	30.745	30.826	30.941
$n_{amine}/m_{amine+water}$	4.078	4.072	4.088	4.059	4.105	4.085	4.069	4.073	4.072	4.093	4.104	4.119
$\alpha, \frac{\text{mol } CO_2}{\text{mol amine}}$	0.461	0.461	0.460	0.449	0.445	0.447	0.423	0.423	0.423	0.493	0.493	0.487

Appendix 8: $BaCl_2$ titration results of CO_2 loadings and concentrations for 30 wt % 4-amino-1-butanol liquid samples.

Sample	s1	s1	s1	s2	s2	s2	s3	s3	s3
C_{HCl}, mol	0.1	0.1	0.1	0.1	0.1	0.1	0.1	0.1	0.1
V_{HCl}, ml	40.188	23.782	21.972	24.854	23.126	23.254	27.612	28.2	25.24
V_{HCl} blank sample, ml	14.892	14.892	14.892	15.59	15.59	15.59	16.652		
C_{NaOH}, mol	0.1	0.1	0.1	0.1	0.1	0.1	0.1		
V_{NaOH}, ml	22.9638	16.9775	15.3295	17.5283	16.4504	16.2621	19.8788	19.8649	17.8183
V_{NaOH}, blank sample, ml	13.8642	13.8642	13.8642	14.6259	14.6259	14.6259	15.0075		
M_{CO2}, g/mol	44.01	44.01	44.01	44.01	44.01	44.01	44.01		
$m_{sample\ loading}$, g	0.586	0.21	0.204	0.235	0.212	0.222	0.233	0.254	0.218
n(CO_2 in sample), mol	0.00086	0.00034	0.00033	0.00037	0.00033	0.00035	0.00039	0.00042	0.00037
n(CO_2 in blank sample), mol	0.00005	0.00005	0.00005	0.00005	0.00005	0.00005	0.00008	0.00008	0.00008
m(CO_2 in blank sample), g	0.00226	0.00226	0.00226	0.00212	0.00212	0.00212	0.00362	0.00362	0.00362
m(CO_2 in sample), g	0.03564	0.01271	0.01236	0.01400	0.01257	0.01326	0.01340	0.01472	0.01271
$M_{amine+water}$, g/mol	0.55036	0.19729	0.19164	0.22100	0.19943	0.20874	0.21960	0.23928	0.20529
$n_{CO2}/m_{amine+water}$	1.47144	1.46402	1.46487	1.43927	1.43194	1.44388	1.38630	1.39808	1.40710
f	0.06082	0.06053	0.06056	0.05957	0.05928	0.05975	0.05750	0.05796	0.05832
C_{amine}, mol	1	1	1	1	1	1	1		
V_{amine}, ml	3.586	3.586	3.586	3.586	3.586	3.586	3.586	3.586	3.586
M_{amine}, g/mol	89.14	89.14	89.14	89.14	89.14	89.14	89.14		
$m_{amine.cons}$, g	0.320	0.320	0.320	0.320	0.320	0.320	0.320	0.320	0.320
$m_{sample.cons}$, g	1.149	1.149	1.149	1.149	1.149	1.149	1.149	1.149	1.149
$m_{amine+water.cons}$, g	1.079	1.079	1.079	1.081	1.081	1.080	1.083	1.082	1.082
wt% amine	29.622	29.613	29.614	29.583	29.574	29.588	29.518	29.532	29.543
$n_{amine}/m_{amine+water}$	3.323	3.322	3.322	3.319	3.318	3.319	3.311	3.313	3.314
$\alpha, \frac{mol\ CO_2}{mol\ amine}$	0.443	0.441	0.441	0.434	0.432	0.435	0.419	0.422	0.425

Appendix 8 (continued)

Sample	s4	s4	s4	s5	s5	s5	s6	s6	s7	s7	s7
C_{HCl}, mol	0.1	0.1	0.1	0.1	0.1	0.1	0.1	0.1	0.1	0.1	0.1
V_{HCl}, ml	24.996	22.56	24.474	21.456	22.42	24.656	22.502	21.922	21.844	23.746	17.72
V_{HCl} blank sample, ml	16.65	16.65	16.65	16.708	16.708	16.708	14.848	14.848	11.809	11.809	11.809
C_{NaOH}, mol	0.1	0.1	0.1	0.1	0.1	0.1	0.1	0.1	0.1	0.1	0.1
V_{NaOH}, ml	18.4446	16.3787	18.1715	15.5317	16.525	18.473	17.7521	16.8786	13.553	15.507	9.15
V_{NaOH}, blank sample, ml	15.9161	15.9161	15.9161	15.4824	15.4824	15.4824	14.2935	14.2935	10.875		
M_{CO2}, g/mol	44.01	44.01	44.01	44.01	44.01	44.01	44.01	44.01	44.01	44.01	44.01
$m_{sample\ loading}$, g	0.231	0.218	0.223	0.214	0.215	0.225	0.268	0.287	0.502	0.5	0.52
n(CO_2 in sample), mol	0.00033	0.00031	0.00032	0.00030	0.00029	0.00031	0.00024	0.00025	0.00041	0.00041	0.00043
n(CO_2 in blank sample), mol	0.00004	0.00004	0.00004	0.00006	0.00006	0.00006	0.00003	0.00003	0.00005	0.00005	0.00005
m(CO_2 in blank sample), g	0.00161	0.00161	0.00161	0.00270	0.00270	0.00270	0.00122	0.00122	0.00206	0.00206	0.00206
m(CO_2 in sample), g	0.01280	0.01199	0.01225	0.01034	0.01028	0.01091	0.00923	0.00988	0.01619	0.01607	0.01680
$M_{amine+water}$, g/mol	0.21820	0.20601	0.21075	0.20366	0.20472	0.21409	0.25877	0.27712	0.48581	0.48393	0.50320
$n_{CO2}/m_{amine+water}$	1.33307	1.32210	1.32116	1.15356	1.14041	1.15778	0.81065	0.80991	0.75719	0.75477	0.75875
f	0.05542	0.05499	0.05495	0.04832	0.04779	0.04848	0.03445	0.03442	0.03225	0.03215	0.03231
C_{amine}, mol	1	1	1	1	1	1	1	1	1	1	1
V_{amine}, ml	3.586	3.586	3.586	3.586	3.586	3.586	3.586	3.586	6.393	6.92	6.577
M_{amine}, g/mol	89.14	89.14	89.14	89.14	89.14	89.14	89.14	89.14	89.14	89.14	89.14
$m_{amine.cons}$, g	0.320	0.320	0.320	0.320	0.320	0.320	0.320	0.320	0.570	0.617	0.586
$m_{sample.cons}$, g	1.149	1.149	1.149	1.149	1.149	1.149	1.149	1.149	2.005	2.162	2.054
$m_{amine+water.cons}$, g	1.085	1.086	1.086	1.093	1.094	1.093	1.109	1.109	1.940	2.092	1.988
wt% amine	29.453	29.439	29.438	29.233	29.217	29.238	28.813	28.812	29.370	29.479	29.496
$n_{amine}/m_{amine+water}$	3.304	3.303	3.302	3.279	3.278	3.280	3.232	3.232	3.295	3.307	3.309
$\alpha, \frac{\text{mol } CO_2}{\text{mol amine}}$	0.403	0.400	0.400	0.352	0.348	0.353	0.251	0.251	0.230	0.228	0.229

Appendix 9: $BaCl_2$ titration results of CO_2 loadings and concentrations for 30 wt % 5-amino-1-pentanol liquid samples.

Sample	s1	s1	s1	s2	s2	s2	s3	s3	s3
C_{HCl}, mol	0.1	0.1	0.1	0.1	0.1	0.1	0.1	0.1	0.1
V_{HCl}, ml	33.667	34.239	32.822	34.787	32.05	35.975	36.038	35.567	36.495
V_{HCl} blank sample, ml	18.704	18.704	18.704	18.704	18.704	18.704	17.853	17.853	17.853
C_{NaOH}, mol	0.1	0.1	0.1	0.1	0.1	0.1	0.1	0.1	0.1
V_{NaOH}, ml	21.046	21.858	20.484	20.069	17.484	21.427	21.942	21.542	22.543
V_{NaOH}, blank sample, ml	17.828	17.828	17.828	17.828	17.828	17.828	17.512	17.512	17.512
M_{CO2}, g/mol	44.01	44.01	44.01	44.01	44.01	44.01	44.01	44.01	44.01
$m_{sample\ loading}$, g	0.41	0.402	0.402	0.5	0.502	0.501	0.505	0.509	0.502
n(CO_2 in sample), mol	0.00063	0.00062	0.00062	0.00074	0.00073	0.00073	0.00070	0.00070	0.00070
n(CO_2 in blank sample), mol	0.00004	0.00004	0.00004	0.00004	0.00004	0.00004	0.00002	0.00002	0.00002
m(CO_2 in blank sample), g	0.00193	0.00193	0.00193	0.00193	0.00193	0.00193	0.00075	0.00075	0.00075
m(CO_2 in sample), g	0.02584	0.02532	0.02522	0.03046	0.03012	0.03009	0.03027	0.03011	0.02995
$M_{amine+water}$, g/mol	0.38416	0.37668	0.37678	0.46954	0.47188	0.47091	0.47473	0.47889	0.47205
$n_{CO2}/m_{amine+water}$	1.52868	1.52715	1.52106	1.47399	1.45060	1.45164	1.44871	1.42873	1.44169
f	0.06304	0.06298	0.06274	0.06092	0.06001	0.06005	0.05994	0.05916	0.05966
C_{amine}, mol	1	1	1	1	1	1	1	1	1
V_{amine}, ml	4.176	4.177	4.206	4.013	4.13	4.134	5.513	4.185	4.227
M_{amine}, g/mol	103.16	103.16	103.16	103.16	103.16	103.16	103.16	103.16	103.16
$m_{amine.cons}$, g	0.431	0.431	0.434	0.414	0.426	0.426	0.569	0.432	0.436
$m_{sample.cons}$, g	1.561	1.566	1.578	1.502	1.542	1.546	2.007	1.551	1.57
$m_{amine+water.cons}$, g	1.463	1.467	1.479	1.411	1.449	1.453	1.887	1.459	1.476
wt% amine	29.454	29.365	29.337	29.350	29.394	29.347	30.144	29.585	29.537
$n_{amine}/m_{amine+water}$	2.855	2.847	2.844	2.845	2.849	2.845	2.922	2.868	2.863
$\alpha, \frac{mol\ CO_2}{mol\ amine}$	0.535	0.536	0.535	0.518	0.509	0.510	0.496	0.498	0.504

Appendix 9 (continued).

Sample	s4	s4	s4	s5	s5	s5	s6	s6	s6
C_{HCl}, mol	0.1	0.1	0.1	0.1	0.1	0.1	0.1	0.1	0.1
V_{HCl}, ml	34.862	33.413	29.656	33.34	36.371	33.883	26.406	32.612	30.498
V_{HCl} blank sample, ml	17.853	17.853	17.853	18.073	18.073	18.073	18.073	18.073	18.073
C_{NaOH}, mol	0.1	0.1	0.1	0.1	0.1	0.1	0.1	0.1	0.1
V_{NaOH}, ml	22.08	20.387	16.67	21.534	24.24	21.972	16.088	22.28	20.048
V_{NaOH}, blank sample, ml	17.512	17.512	17.512	17.521	17.521	17.521	17.521	17.521	17.521
M_{CO2}, g/mol	44.01	44.01	44.01	44.01	44.01	44.01	44.01	44.01	44.01
$m_{sample\ loading}$, g	0.5	0.503	0.501	0.5	0.512	0.506	0.506	0.503	0.501
n(CO_2 in sample), mol	0.00064	0.00065	0.00065	0.00059	0.00061	0.00060	0.00052	0.00052	0.00052
n(CO_2 in blank sample), mol	0.00002	0.00002	0.00002	0.00003	0.00003	0.00003	0.00003	0.00003	0.00003
m(CO_2 in blank sample), g	0.00075	0.00075	0.00075	0.00121	0.00121	0.00121	0.00121	0.00121	0.00121
m(CO_2 in sample), g	0.02738	0.02791	0.02783	0.02476	0.02548	0.02500	0.02149	0.02152	0.02178
$M_{amine+water}$, g/mol	0.47262	0.47509	0.47317	0.47524	0.48652	0.48100	0.48451	0.48148	0.47922
$n_{CO2}/m_{amine+water}$	1.31616	1.33502	1.33619	1.18404	1.18998	1.18076	1.00782	1.01562	1.03272
f	0.05475	0.05549	0.05554	0.04953	0.04976	0.04940	0.04247	0.04279	0.04347
C_{amine}, mol	1	1	1	1	1	1	1	1	1
V_{amine}, ml	5.495	5.397	5.388	5.491	5.532	5.517	5.664	5.567	5.566
M_{amine}, g/mol	103.16	103.16	103.16	103.16	103.16	103.16	103.16	103.16	103.16
$m_{amine.cons}$, g	0.567	0.557	0.556	0.566	0.571	0.569	0.584	0.574	0.574
$m_{sample.cons}$, g	2.043	2.004	2.004	2.01	2.03	2.021	2.035	2.005	2.004
$m_{amine+water.cons}$, g	1.931	1.893	1.893	1.910	1.929	1.921	1.949	1.919	1.917
wt% amine	29.354	29.414	29.367	29.650	29.585	29.624	29.986	29.923	29.954
$n_{amine}/m_{amine+water}$	2.845	2.851	2.847	2.874	2.868	2.872	2.907	2.901	2.904
$\alpha, \frac{mol\ CO_2}{mol\ amine}$	0.463	0.468	0.469	0.412	0.415	0.411	0.347	0.350	0.356

Appendix 9 (continued).

Sample	s7	s7	s7	s8	s8	s8
C_{HCl}, mol	0.1	0.1	0.1	0.1	0.1	0.1
V_{HCl}, ml	30.598	31.158	29.943	25.197	26.544	26.806
V_{HCl} blank sample, ml	16.503	16.503	16.503	16.503	16.503	16.503
C_{NaOH}, mol	0.1	0.1	0.1	0.1	0.1	0.1
V_{NaOH}, ml	23.066	23.304	21.792	15.853	17.295	17.377
V_{NaOH}, blank sample, ml	15.891	15.891	15.891	15.891	15.891	15.891
M_{CO2}, g/mol	44.01	44.01	44.01	44.01	44.01	44.01
$m_{sample\ loading}$, g	0.508	0.506	0.508	0.506	0.503	0.513
n(CO_2 in sample), mol	0.00038	0.00039	0.00041	0.00047	0.00046	0.00047
n(CO_2 in blank sample), mol	0.00003	0.00003	0.00003	0.00003	0.00003	0.00003
m(CO_2 in blank sample), g	0.00135	0.00135	0.00135	0.00135	0.00135	0.00135
m(CO_2 in sample), g	0.01523	0.01594	0.01659	0.01921	0.01901	0.01940
$M_{amine+water}$, g/mol	0.49277	0.49006	0.49141	0.48679	0.48399	0.49360
$n_{CO2}/m_{amine+water}$	0.70215	0.73888	0.76708	0.89690	0.89226	0.89314
f	0.02998	0.03149	0.03266	0.03797	0.03778	0.03782
C_{amine}, mol	1	1	1	1	1	1
V_{amine}, ml	5.646	5.754	5.643	5.625	5.637	5.637
M_{amine}, g/mol	103.16	103.16	103.16	103.16	103.16	103.16
$m_{amine.cons}$, g	0.582	0.594	0.582	0.580	0.582	0.582
$m_{sample.cons}$, g	2.009	2.046	2.005	2.009	2.014	2.014
$m_{amine+water.cons}$, g	1.949	1.982	1.940	1.933	1.938	1.938
wt% amine	29.887	29.955	30.014	30.024	30.007	30.008
$n_{amine}/m_{amine+water}$	2.897	2.904	2.909	2.910	2.909	2.909
$\alpha, \frac{mol\ CO_2}{mol\ amine}$	0.242	0.254	0.264	0.308	0.307	0.307